

This is an Open Access document downloaded from ORCA, Cardiff University's institutional repository: <https://orca.cardiff.ac.uk/id/eprint/107116/>

This is the author's version of a work that was submitted to / accepted for publication.

Citation for final published version:

Abd El-wahab, Hend A.A., Accietto, Mauro, Marino, Leonardo B., McLean, Kirsty J., Levy, Colin W., Abdel-Rahman, Hamdy M., El-Gendy, Mahmoud A., Munro, Andrew W., Aboraia, Ahmed S. and Simons, Claire 2018. Design, synthesis and evaluation against Mycobacterium tuberculosis of azole piperazine derivatives as dicyclotyrosine (cYY) mimics. *Bioorganic & Medicinal Chemistry* 26 (1) , pp. 161-176. 10.1016/j.bmc.2017.11.030

Publishers page: <http://dx.doi.org/10.1016/j.bmc.2017.11.030>

Please note:

Changes made as a result of publishing processes such as copy-editing, formatting and page numbers may not be reflected in this version. For the definitive version of this publication, please refer to the published source. You are advised to consult the publisher's version if you wish to cite this paper.

This version is being made available in accordance with publisher policies. See <http://orca.cf.ac.uk/policies.html> for usage policies. Copyright and moral rights for publications made available in ORCA are retained by the copyright holders.



Design, synthesis and evaluation against *Mycobacterium tuberculosis* of azole piperazine derivatives as dicyclotyrosine (cYY) mimics

Hend A.A. Abd El-wahab,^{a,b} Mauro Accietto,^{a,c} Leonardo B. Marino,^d Kirsty J. McLean,^e Colin W Levy,^e Hamdy M. Abdel-Rahman,^b Mahmoud A. El-Gendy,^b Andrew W. Munro,^e Ahmed S. Aboaraia,^b and Claire Simons^{a*}

^aSchool of Pharmacy and Pharmaceutical Sciences, Cardiff University, Cardiff CF10 3NB, Wales, UK

^bDepartment of Medicinal Chemistry, Faculty of Pharmacy, Assiut University, Assiut 71526, Egypt

^cDepartment of Life Sciences, University of Modena and Reggio Emilia, Via G. Campi 183, 41125 Modena, Italy

^dFaculty of Pharmaceutical Sciences, UNESP - Univ Estadual Paulista, Araraquara, São Paulo 14801-902, Brazil.

^eManchester Institute of Biotechnology, School of Chemistry, University of Manchester, Manchester M1 7DN

* Address for correspondence: Claire Simons, School of Pharmacy and Pharmaceutical Sciences, Cardiff University, Redwood Building, King Edward VII Avenue, Cardiff CF10 3NB, Wales, UK. Tel: 02920-876307. E-mail: simonsc@cardiff.ac.uk

Abstract

Three series of azole piperazine derivatives that mimic dicyclotirosine (cYY), the natural substrate of the essential *Mycobacterium tuberculosis* cytochrome P450 CYP121A1, were prepared and evaluated for binding affinity and inhibitory activity (MIC) against *M. tuberculosis*. Series A replaces one phenol group of cYY with a C3-imidazole moiety, series B includes a keto group on the hydrocarbon chain preceding the series A imidazole, whilst series C explores replacing the keto group of the piperidone ring of cYY with a CH₂-imidazole or CH₂-triazole moiety to enhance binding interaction with the heme of CYP121A1. The series displayed moderate to weak type II binding affinity for CYP121A1, with the exception of series B **10a**, which displayed mixed type I binding. Of the three series, series C imidazole derivatives showed the best, although modest, inhibitory activity against *M. tuberculosis* (**17d** MIC = 12.5 µg/mL, **17a** 50 µg/mL). Crystal structures were determined for CYP121A1 bound to series A compounds **6a** and **6b** that show the imidazole groups positioned directly above the haem iron with binding between the haem iron and imidazole nitrogen of both compounds at a distance of 2.2 Å. A model generated from a 1.5 Å crystal structure of CYP121A1 in complex with compound **10a** showed different binding modes in agreement with the heterogeneous binding observed. Although the crystal structures of **6a** and **6b** would indicate binding with CYP121A1, the binding assays themselves did not allow confirmation of CYP121A1 as the target.

Keywords

Dicyclotirosine derivatives; CYP121A1; *Mycobacterium tuberculosis*; binding affinity; molecular modeling; X-ray crystallography

1. Introduction

Tuberculosis (TB) is an infectious, communicable bacterial disease, most commonly of the respiratory tract, usually caused by *Mycobacterium tuberculosis* (Mtb).¹ Despite the 47% mortality rate reduction (1990-2014), case numbers are rising in developing countries with 1.8 million deaths from TB in 2015.² An estimated 480,000 people developed multi-drug resistant TB (MDR-TB) in 2015.² The rise in MDR-TB, a form of TB caused by bacteria that do not respond to isoniazid and rifampicin,³ the two most effective first-line TB drugs, is alarming and highlights the need for the identification of new drug targets.

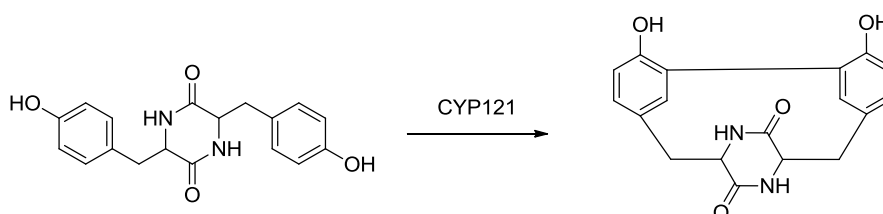


Figure 1. Formation of mycocyclosin. *M. tuberculosis* CYP121A1 catalyses the oxidative crosslinking of the aryl side chains of the cyclic dipeptide, cyclo-*L*-Tyr-*L*-Tyr (cYY), to produce the novel secondary metabolite mycocyclosin.

A potential new target is the cytochrome P450 enzyme CYP121A1 that was shown to be essential for mycobacterial growth through gene deletion and complementation studies.⁴ The natural substrate of CYP121A1 is the cyclic dipeptide (CDP) dicycloxyrosine (cYY) and it was found that CYP121A1 exhibits a novel diketopiperazine modifying activity, catalysing the formation of a C-C bond between the two tyrosyl side chains of cYY resulting in a novel chemical entity called mycocyclosin (Figure 1). The role of the secondary metabolite mycocyclosin in *M. tuberculosis* remains unclear, although CDPs and their derivatives have important biological effects, including (i) cFP in the bacterial pathogen *Vibrio cholerae*, production of which inhibits production of bacterial virulence factors, (ii) cLY which

can inhibit biofilm formation in the skin bacterium *Staphylococcus epidermidis*; and cHP which has reported neuroprotective effects in mammals.⁵⁻⁷

Recent studies revealed that only cyclodipeptides with a diketopiperazine ring and two aryl side chains with L-configuration bound well to CYP121A1, and that only cYY itself was efficiently transformed to a product.^{8,9}

The binding of cYY to CYP121A1 includes a direct hydrogen bond interaction between the carbonyl of cYY and the side chain nitrogen of Asn85, and a water-mediated hydrogen bonding pattern. Hydrophobic interactions are demonstrated on the other side chain (Figure 2). The CDP cYY is a small molecule that partially occupies (300 Å) the large active site cavity (1350 Å³) of CYP121A1, and makes several interactions with P450 amino acids, both directly and via interstitial active site water molecules.⁹

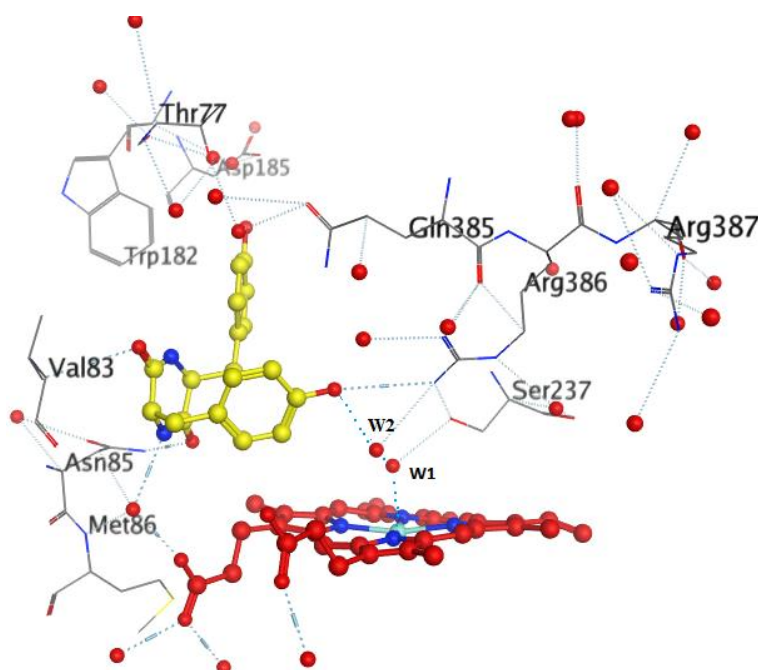


Figure 2. Crystal structure of cYY bound to CYP121A1. cYY is shown with carbon atoms in yellow, and with interactions between cYY and active site amino acids and water molecules shown with dotted lines. cYY shows indirect binding coordination of the CYP121A1 heme iron through an axial water molecule (red) to the heme iron (cyan) (pdb code: 3G5H).

Three small series that mimic the natural substrate cYY have been developed (Figure 3). Series A replaces one of the phenol rings of cYY, which is positioned directly above the heme group in the crystal structure (Figure 2), for a C3-imidazole. Flexible alignment showed that the three carbon chain allowed optimal overlap of the imidazole ring with the phenol ring (Figure 3). Also in this series, the central piperazine ring retains the planar conformation of cYY.

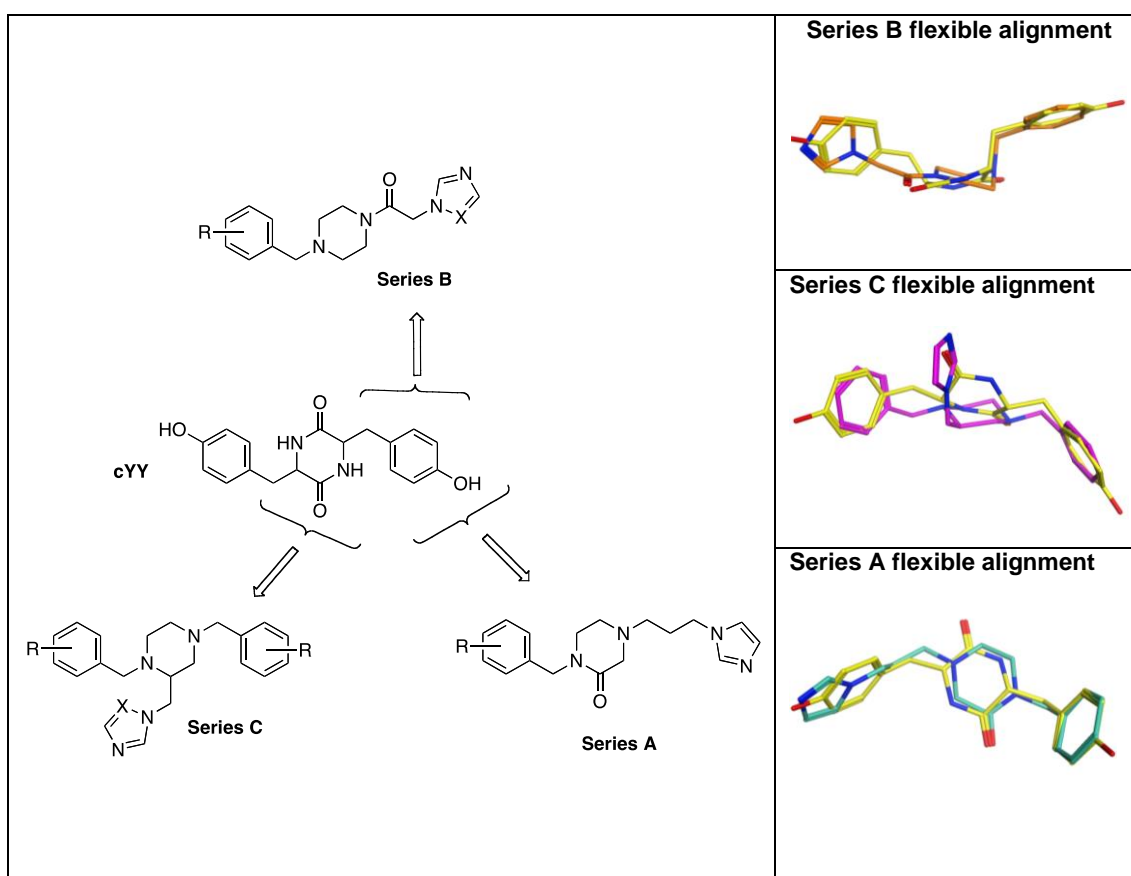


Figure 3. Designed cYY mimics from series A, B and C. Flexible alignment of cYY (yellow) with series A (cyan), series B (orange) and series C (magenta).

Series B includes a keto group on the hydrocarbon chain preceding the series A imidazole. The rationale for this modification of series B was to mimic the piperazine keto group, and the shorter two carbon chain, attached to a piperidine ring with more conformational flexibility, that was a sufficient length to allow overlap of the imidazole with the phenol ring (Figure 3). Series 3 is perhaps the closest mimic retaining two aromatic rings, although it has the piperazine ring with more

conformational flexibility, as with series B. In Series C the keto group of the piperidone ring of cYY is replaced by a CH₂-imidazole or CH₂-triazole, to determine whether a direct interaction between the inhibitor compound and the heme group might place the inhibitor more optimally within the active site.

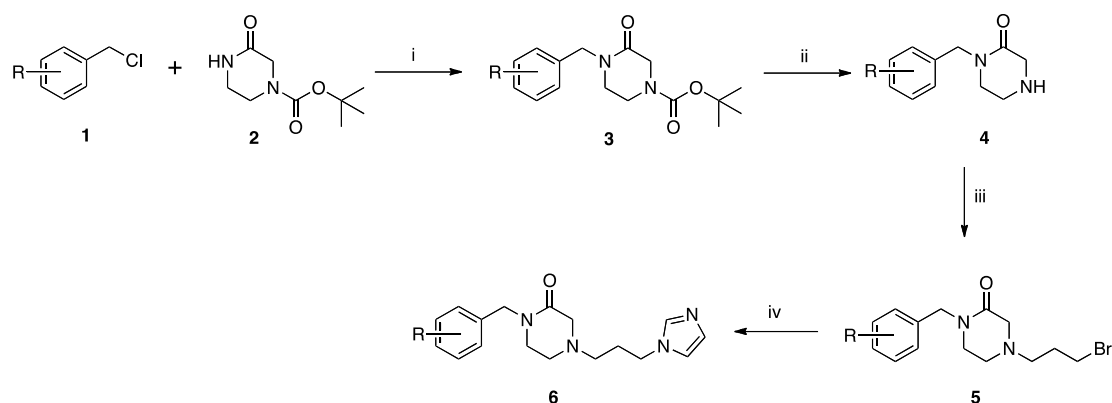
The choice of imidazole and triazole as the haem-binding heterocycles was based on previous binding studies,^{10,11} which showed that the imidazole interacts optimally through a N:-Fe^{III}-haem coordinate link, through the N3 of imidazole, while introducing an additional nitrogen in the heterocyclic ring (triazole) reduces the coordination potential through the N: due to the electron withdrawing effect of the additional electronegative nitrogen. This effect is further increased with two additional nitrogens (tetrazole) drawing electron density from both sides of the coordinating nitrogen. Although the triazole is expected to have a lower binding affinity for the haem iron, the lower basicity of the triazole can confer greater isoform-specific selectivity in various CYP enzymes.¹²

2. Results and discussion

2.1 Chemistry

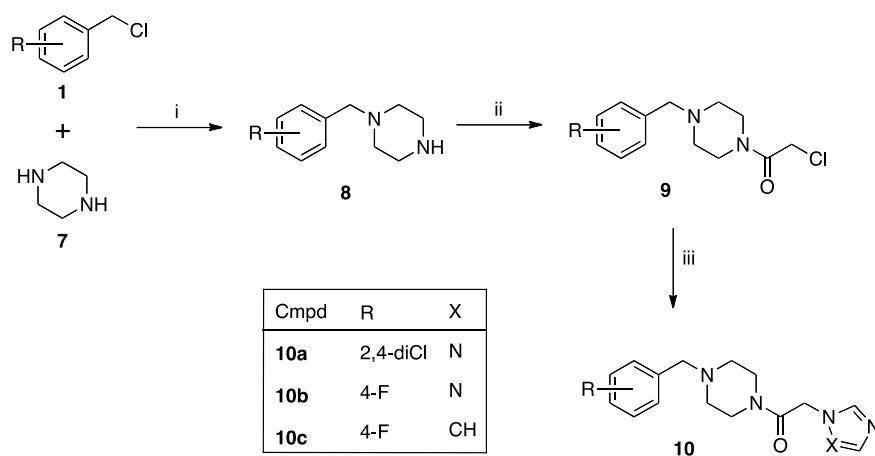
Series A began with the preparation of the 4-(substituted)-3-oxo-piperazine-1-carboxylic acid *tert*-butyl esters (**3**) according to the literature procedure¹³ by addition of the substituted benzyl chlorides (**1**) to a solution of 1-Boc-3-oxopiperazine (**2**) in anhydrous DMF in the presence of NaH (Scheme 1). Deprotection of the Boc protecting group of (**3**) was achieved using 4 M HCl solution in dioxane to obtain the piperazine (**4**) in very good yields. Treatment of 1-(substituted)-piperazin-2-one (**4**) with K₂CO₃ and dibromopropane for 48 h gave the alkylated products (**5**) after purification by flash column chromatography.¹⁴ Reaction of 4-(bromopropyl)-1-(4-

substituted-benzyl)-piperazin-2-ones (**5**) with the sodium salt of imidazole gave the final imidazole products (**6**) in moderate yields (Scheme 1).



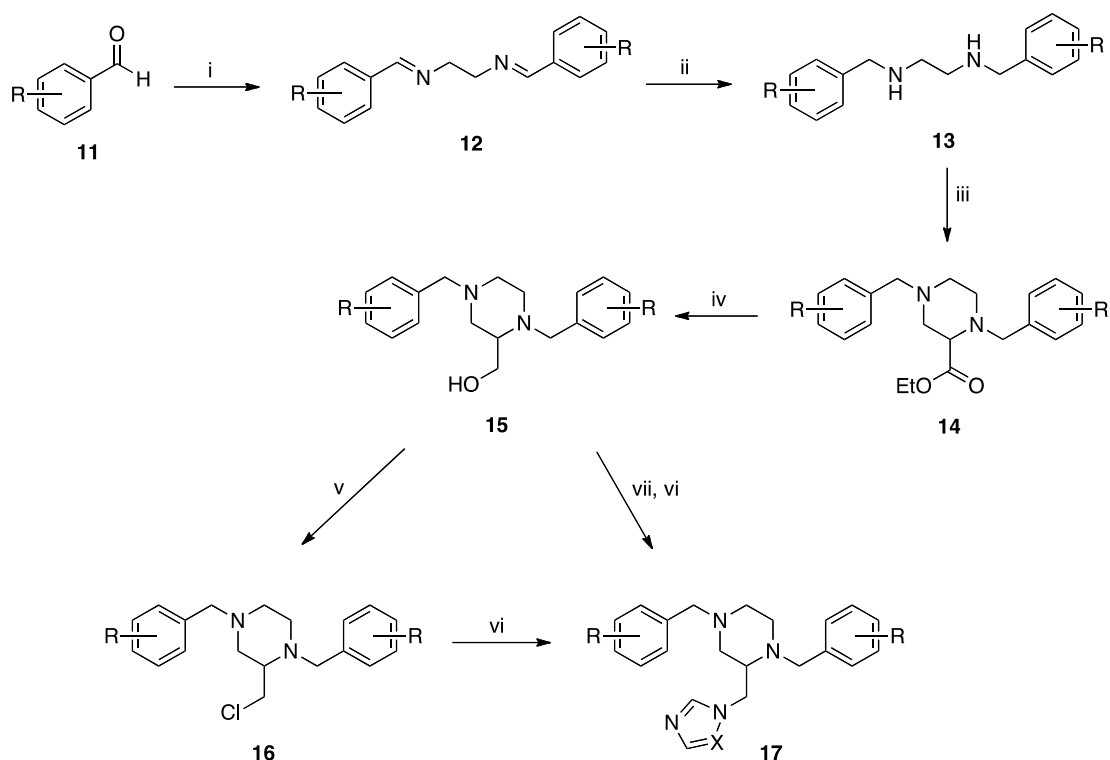
Scheme 1. *Reagents and conditions:* (i) NaH, DMF, 70 °C, o/n (ii) 4 M HCl, dioxane, o/n (iii) K₂CO₃, acetone, Br(CH₂)₃Br, 48 h (iv) imidazole, NaH, DMF, 45 °C, o/n. [**a**, R = 4-F; **b**, R = 4-Cl; **c**, R = 4-OCH₃; **d**, R = 2,4-diCl]

Series B began with the preparation of 1-(substituted-benzyl)piperazine (**8**) by addition of substituted benzyl chloride (**1**) to a solution of excess piperazine (**7**) in anhydrous THF. Treatment of the formed 1-(substituted-benzyl)piperazine (**8**) with triethylamine and 2-chloroacetyl chloride gave the acylated products (**9**),¹⁵ which were pure enough to proceed for the next step. The final compounds (**10**) were prepared by reaction of the acylated products (**9**) with 1,2,4-triazole or imidazole in the presence of K₂CO₃ (Scheme 2).



Scheme 2. *Reagents and conditions:* (i) THF, 70 °C, 2.5 h (ii) 2-chloroacetylchloride, Et₃N, 0°C, 2 h then rt 5 h (iii) K₂CO₃, CH₃CN, imidazole or triazole, 45 °C, 1 h then **9**, 70 °C, o/n.

For Series C the substitutions were limited to unsubstituted and methoxy groups. The methoxy substituents were included as H-bond acceptors to mimic the phenolic hydroxyl of the tyrosine group of cYY. The imines (**12**) were prepared by reaction of ethylenediamine and the desired benzaldehyde (**11**) in ethanol overnight at room temperature (Scheme 3). Subsequent reduction of the imines (**12**)¹⁶ with NaBH₄ gave the diamines (**13**)¹⁷, which on reaction with 2,3-dibromopropionic acid ethyl ester and triethylamine in toluene at 80 °C resulted in cyclisation to the piperazine esters (**14**). Ester reduction was performed using LiAlH₄ giving the corresponding alcohols (**15**). The unsubstituted and 4-methoxy derivatives **15a** and **15b** were then converted to the chlorides (**16a** and **16b**) on reaction with thionyl chloride at reflux overnight. Attempts to convert the dimethoxy alcohol (**15c**) to the chloride were unsuccessful with a complex reaction mixture obtained, and therefore the dimethoxy alcohol (**15c**) was first converted to the mesylate intermediate by reaction with methanesulphonyl chloride in the presence of base (Et₃N). Treatment of the chlorides and mesylate with either the sodium salt of imidazole or triazole generated *in situ* on reaction of imidazole and triazole, respectively, with NaH in acetonitrile or toluene, gave the final imidazole and triazole compounds (**17**) (Scheme 3).



Scheme 3. *Reagents and conditions:* (i) H₂NCH₂CH₂NH₂, EtOH, o/n (ii) NaBH₄, MeOH, o/n (iii) 2,3-dibromopropionic acid ethyl ester, toluene, Et₃N, 80 °C, o/n (iv) LiAlH₄, Et₂O, o/n (v) SOCl₂, toluene, 115 °C, o/n (vi) NaH, imidazole or triazole, CH₃CN, 80 °C, o/n (vii) MsCl, Et₃N, CH₂Cl₂, 4 h (vii) NaH, imidazole, toluene, 115 °C, o/n. [**a**, R = H, X = CH; **b**, R = H, X = N; **c**, R = 4-OCH₃, X = N; **d**, R = 3,5-diOCH₃, X = CH]

2.2 Binding affinity

UV–visible absorption spectroscopy is an important technique for the characterization and quantification of cytochrome P450 enzymes, including the assessment of whether an applied ligand is a likely substrate or inhibitor, based on it causing a heme Soret band blue or red shift, respectively. The oxidized form of pure CYP121A1 shows spectral properties that are similar to those of many other predominantly low-spin P450 enzymes, with the major (Soret or γ) ferric heme band located at 416 nm (most P450s have the low-spin Soret feature at ~418-419 nm), and the smaller α and β bands at 565 and 538 nm, respectively. On reduction of CYP121A1 with sodium dithionite and binding of carbon monoxide at basic pH, the Soret band shifts to 448

nm with a small decrease in intensity, confirming that cysteine thiolate coordination is retained in the Fe^{II}-CO state (Figure 4).¹⁸

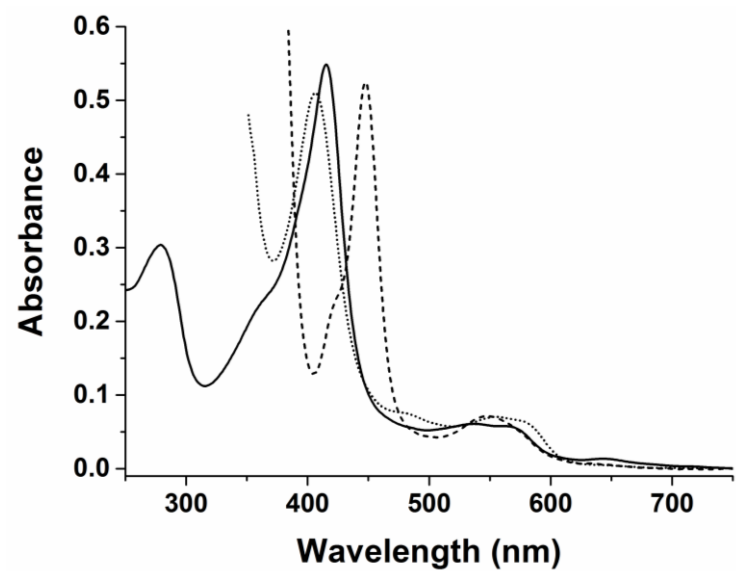
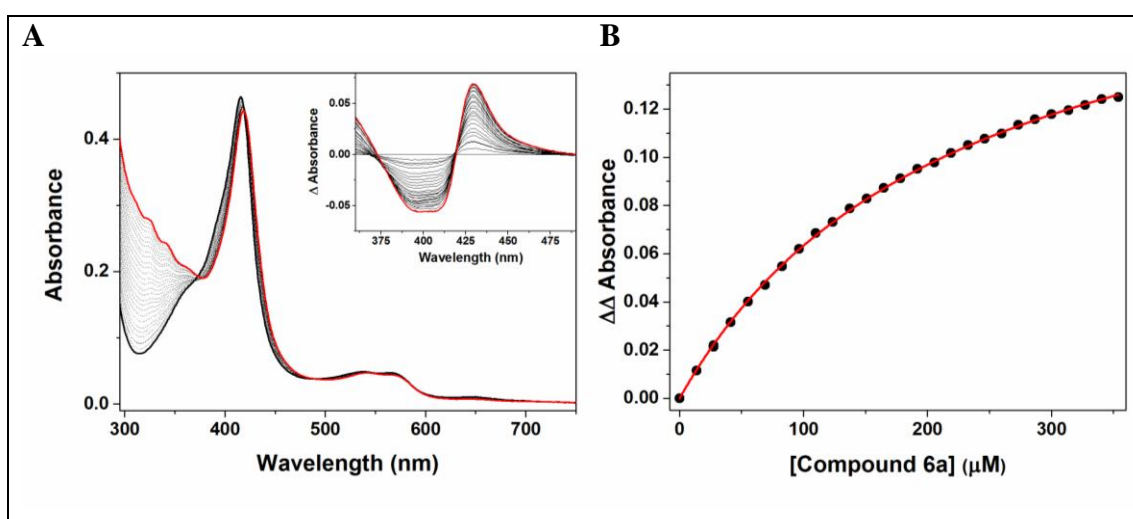


Figure 4: Spectroscopic characteristics of CYP121A1. CYP121A1 (solid line, 5.2 μ M) in the normal low-spin resting form with Soret peak at 416nm and α and β bands at 565 and 538 nm, respectively. CYP121A1 retains a small degree of high-spin with a charge transfer band at 649 nm and small Soret shoulder at 394 nm. Reduction with sodium dithionite (dotted line) shows a decrease in intensity of the Soret peak and shift to 406 nm with fusion of the α and β bands to a new peak at 547nm. Addition of carbon monoxide to reduced CYP121A1 shows the characteristic ‘P450’ peak at 448 nm.

Binding titrations were carried out for compounds **6** (series A), **10** (series B) and **17** (series C). Results shown in Table 1 revealed that compounds from series A, B and C produce small spectral changes and produce moderate to high dissociation constants using either a hyperbolic fit or the Hill function in cases where the data were sigmoidal in nature. Addition of all the compounds (with the exception of **10a**) showed a type II (inhibitor-like) red shift in the heme Soret peak to a longer wavelength, indicating binding of the azole (or triazole) nitrogen to the heme iron (Figure 5). Series A displays the tightest binding with lowest K_d values determined in

particular for the halogenated compound **6b** (4-Cl group, $K_d = 81.3 \pm 2.9 \mu\text{M}$) and compound **6a** (4-F group, $K_d = 225.8 \pm 2.6 \mu\text{M}$). Interestingly, the triazole-containing 2-4-dichloro derivative compound **10a** displays a heterogeneity in binding mode with the development of a blue-shifted high spin type I (substrate-like) shoulder at 393 nm that is accompanied by the appearance of a small charge transfer species at 648 nm, which is also associated with substrate-like binding. In contrast, the remaining Series B and C compounds display small type II inhibitor like spectral changes upon binding to CYP121A1 (Figure 5). The binding of compounds **6b**, **6c** and **10a** to CYP121A1 was best fitted using the Hill function. The apparent cooperative nature of the binding of these ligands may suggest that more than one molecule of these compounds can enter the CYP121A1 active site, or e.g. that there are interactions between CYP121A1 proteins that influence binding affinity. Such phenomena are relatively common in P450 enzymes, as described by Korzekwa *et al.*¹⁹



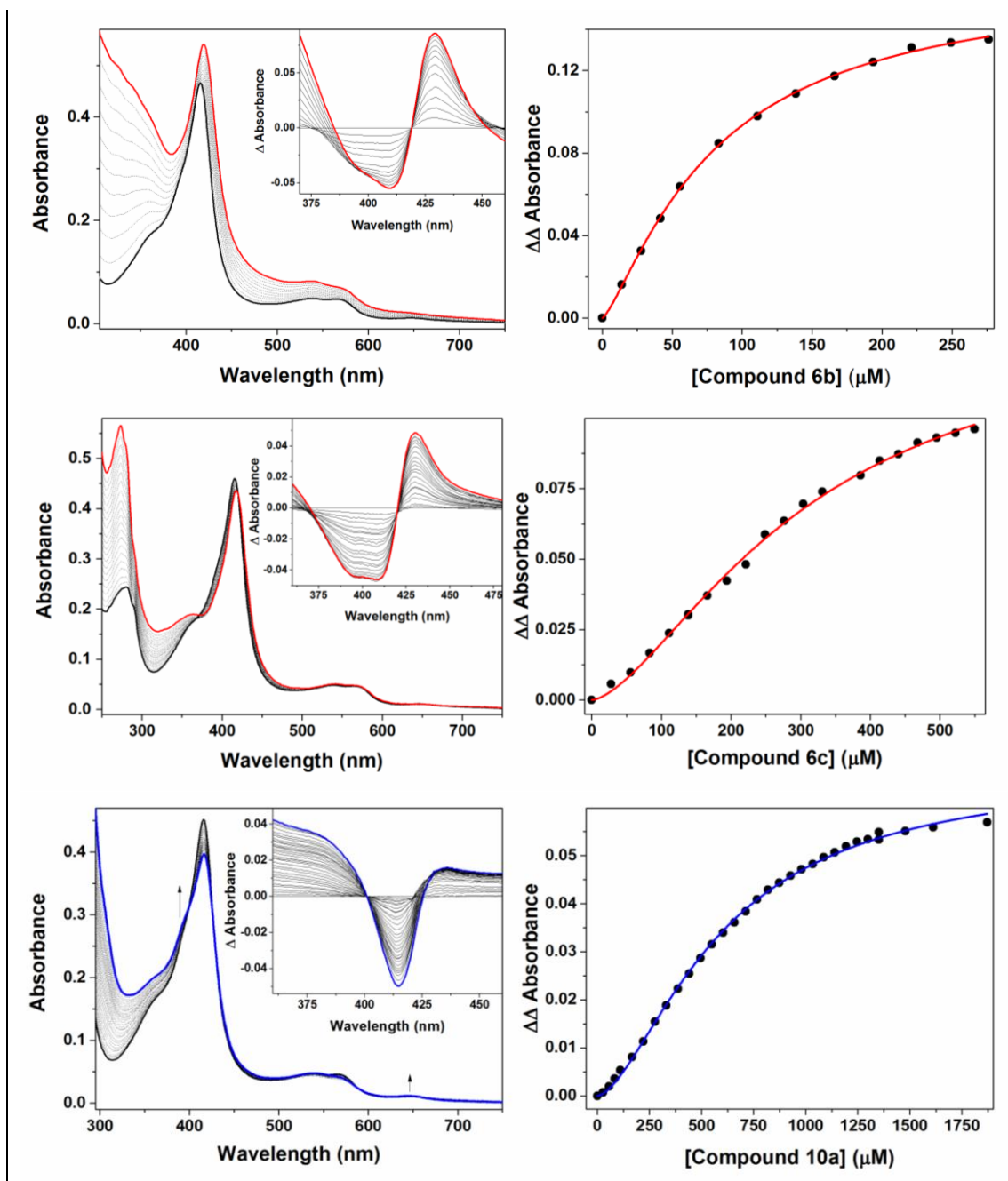


Figure 5. CYP121A1 titrations with selected novel ligands. (A) Spectral titration data for CYP121A1 with various ligands designed and synthesized in this study. Most ligands produce a type II spectral shift indicative of direct or indirect (e.g. via H₂O molecule(s)) interactions of these ligands with the P450 heme iron. The exception shown here is molecule **10a**, which induces a type I spectral change indicative of substrate-like P450 behaviour. (B) Data plots for each ligand, fitted using either hyperbolic (Michaelis-Menten) or sigmoidal (Hill) functions. Data for compound 6a were best fitted using the hyperbolic function, while data for compounds **6b**, **6c** and **10a** were fitted using the Hill function.

Azole antifungal drugs (clotrimazole, econazole, fluconazole, ketoconazole and miconazole) were found to bind tightly to Mtb CYP121A1 inducing a shift of the

soret peak to 423.5 nm. The K_d values for clotrimazole, econazole and miconazole are $< 0.2 \mu\text{M}$ indicating tight binding. Fluconazole a triazole compound, showed weaker binding with a K_d value $8.6 \pm 0.2 \mu\text{M}$, while the imidazole-containing clotrimazole showed much higher affinity than fluconazole with a K_d value of $0.07 \pm 0.01 \mu\text{M}$, as determined from a fit to the Morrison equation (Table 1).¹⁸ The natural substrate cYY has a K_d value of $5.82 \pm 0.16 \mu\text{M}$.

Table 1. K_d , MIC data and calculated LogP for series A and series B

Compound	R	X	K_d (μM)	MIC90 ($\mu\text{g/mL}$)	cLogP ^a
6a	4-F	-	225.8 ± 2.6	>100	1.19
6b	4-Cl	-	81.3 ± 2.9	>100	1.59
6c	4-OCH ₃	-	308.9 ± 21.8	>100	0.91
6d	2,4-diCl	-	967.1 ± 41.3	100	2.15
10a	2,4-diCl	N	417 ± 39	>100	1.63
10b	4-F	N	960 ± 62	>100	1.33
10c	4-F	CH	1142 ± 144	>100	1.88
17a	H	CH	1968 ± 137	50	3.56
17b	H	N	1834 ± 62	>100	3.06
17c	4-OCH ₃	N	1298 ± 124	100	2.81
17d	3,5-diOCH ₃	CH	1435 ± 94	12.5	3.05
Fluconazole ¹⁵	-	-	8.6 ± 0.2	>100	0.87
Clotrimazole ¹⁵	-	-	0.07 ± 0.01	0.1	5.97
cYY	-	-	5.82 ± 0.16	-	1.26

a. Crippen's fragmentation²¹

2.3 EPR spectroscopy of ligand binding to CYP121A1

X-band EPR spectroscopy provides important information on P450 heme iron coordination environment and any heterogeneity therein. EPR studies were done for

CYP121A1 in the ligand-free state and in complex with the compounds from series A, B and C.

Table 2. X-band EPR spectra of CYP121A1 in its ligand-free form and for complexes with ligands from series A, B and C.

CYP121A1 ligand/additive	High-spin (HS) g-values	Low-spin (LS) g-values	% HS
No additive	7.94, 3.59	2.49, 2.25, 1.89	2.5
DMSO	7.94, 3.58	2.49, 2.25, 1.89	2.5
6a	7.94, 3.48	2.46, 2.26, 1.90	1.2
6b	7.94, 3.43	2.46, 2.26, 1.90	1.3
6c	7.96	2.47, 2.26, 1.90	1.2
6d	7.97	2.45, 2.26, 1.90	1.2
10a	7.92, 3.61, 1.70	2.47 (sh. 2.41), 2.26, 1.90	22
10b	7.96, 3.51	2.47, 2.26, 1.90	1.3
10c	7.96, 3.48	2.47, 2.26, 1.89	1.2
17a	7.95, 3.58	2.47, 2.26, 1.89	1.2
17b	7.96, 3.54	2.47, 2.26, 1.89	1.3
17c	7.95, 3.52	2.47, 2.26, 1.90	1.1
17d	7.95, 3.44	2.47, 2.26, 1.90	1.1
cYY	8.05, 3.44	2.46, 2.25, 1.90	2.9
Fluconazole	7.94, 3.58	2.45, 2.26, 1.90	2.5

The g-values for the LS and HS forms of CYP121A1 are indicated in each case with the percentage high-spin (HS) in each sample calculated from integration of the spectral peaks. The g-values are given as $g_z/g_y/g_x$ for both the LS and HS components. The HS g_x signal is too weak to be resolved clearly in most samples. The low intensity of the g_y signal also precludes its accurate positioning in the case of compounds **6c** and **6d**. The “sh.” in the case of compound **10a** indicates a shoulder feature at $g_z = 2.41$ on the main g_z value at 2.47.

Ligand-free CYP121A1 has a major rhombic LS spectrum with g-values at 2.49 (g_z), 2.25 (g_y) and 1.85 (g_x) (2.49/2.25/1.85), consistent with a dominant axial coordination

state from cysteine thiolate (proximal) and water (distal) ligands. In addition to the LS signal, there is a small proportion of HS heme retained in CYP121A1, with g -values at 7.94 and 3.59 (Table 2, Figure 6). This small HS signal is consistent with the native CYP121A1 UV-Vis spectrum (Figure 4). EPR analyses of CYP121A1 in complex with the compounds, with the exception of the series B compound **10a**, revealed subtle perturbations in the EPR spectrum, with ~50% decreases in the HS spectral component and a slight narrowing of the LS signal with g -values of the 2.46(2.47)/2.26/1.90 (c.f. cYY 2.46, 2.25, 1.90)⁸.

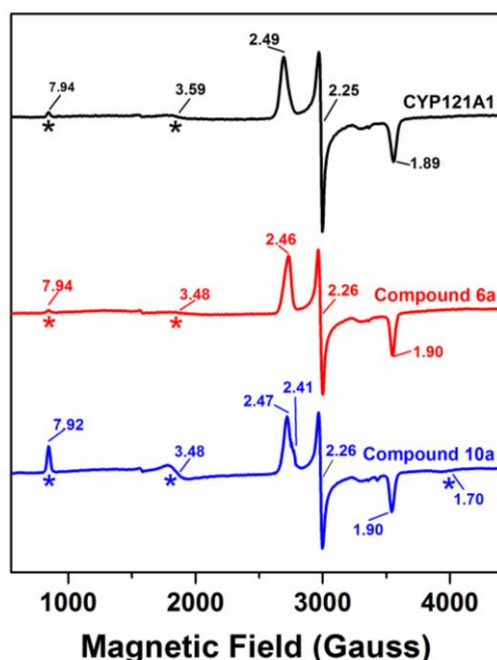


Figure 6. X-band EPR spectra for CYP121A1 in the ligand-free form and when bound to compounds **6a** and **10a**. The g -values are indicated for each peak with HS signals labelled with an asterisk.

These results are not immediately indicative of direct coordination of the heme iron by nitrogen atoms in these molecules, although indirect ligation (via H₂O molecule(s)) cannot be ruled out. In contrast, the addition of compound **10a** displayed a significant perturbation of the EPR spectrum with a 9-fold increase in the amount of HS ferric heme iron (Table 2). A small degree of heterogeneity in the LS signal was also observed, with the formation of a shoulder in the LS g_z signal at 2.41 suggesting

a different binding mode for this ligand in the CYP121A1 active site. Selected EPR spectra are shown in Figure 6.

2.4 Antimycobacterial assay

The derivatives of series A, B and C were screened against Mtb H37Rv by the REMA (Resazurin Microtiter Assay) method.²⁰ In series A only compound **6d** displayed inhibitory activity against *M. tuberculosis* (Table 1) and compounds from Series B were inactive (all >100 µg/mL). Series C was more promising with inhibitory activity observed for three of the derivatives, and with notable activity for the imidazole derivatives **17a** and **17d** (50 and 12.5 µg/mL respectively). There would appear to be a correlation between lipophilicity (cLogP, Table 1) and antimycobacterial activity, which might be explained by enhanced uptake across the lipid dense outer mycobacterial cell wall.

2.5 Crystallography and Molecular Modelling

The structures of CYP121A1 in complex with compounds **6a** and **6b** were solved to 1.64 and 1.5 Å, respectively (PDB codes 5O4L and 5O4K) (Table 3). Compound **6a** and **6b** both sit in a very similar position within the CYP121A1 active site with the imidazole nitrogen coordinated to the heme iron at a distance of 2.2 Å in both cases (Figure 6). A direct H-bond interaction between the keto group of the piperazine ring and Asn85 is observed. In addition, water-bridged H-bonds are formed between the protonated piperazine amine and Met62, Val82 and Val83, and between the piperazine ring and propyl chain linker and Ala233, Gln385 and Arg386. The observed interactions of **6a** and **6b** closely mimic the interactions observed with cYY binding (Figure 2).

Table 3. X-ray crystallography data collection and final structural refinement statistics for CYP121A1 in complex with compounds **6a** and **6b**.

Data Collection and Refinement ^a	CYP121A1/ 6a complex PDB ID 5O4L	CYP121A1/ 6b complex PDB ID 5O4K
Data Collection		
Wavelength (Å)	0.9795	0.9795
Space group	P6 ₅ 22	P6 ₅ 22
Cell dimensions		
a, b, c (Å)	77.53, 77.53, 264.95	77.625, 77.625, 264.291
α , β , γ (°)	90.0, 90.0, 120.0	90.0, 90.0, 120.0
Resolution (Å)	65.09 - 1.64 (1.70 - 1.64)	47.12 - 1.5 (1.56 - 1.5)
Unique reflections	58784 (5714)	76451 (7498)
Multiplicity	19 (20)	19 (20)
Completeness (%)	100 (100)	100 (100)
Mean I/ σ (I)	12.5(1.7)	18.1 (3.0)
Wilson B-factor (Å ²)	20.3	16.1
R-merge	16.9	11.1
R-meas	17.7	11.5
R-pim	4.1	2.6
Refinement		
CC1/2	0.99 (0.49)	0.99 (0.91)
No. Reflections (unique)	58784 (5714)	76444 (7497)
No. Reflections (R-free)	2000 (195)	1993 (195)
R-work	0.18 (0.33)	0.16 (0.24)
R-free	0.20 (0.34)	0.19 (0.26)
No. non-hydrogen atoms	3588	3719
macromolecules	3115	3128
ligands	71	81
solvent	402	510
Protein residues	394	394
RMS(bonds)	0.016	0.019
RMS(angles)	1.66	1.92
Ramachandran favored (%)	99	99
Ramachandran allowed (%)	0.5	0.98
Ramachandran outliers (%)	0	0
Rotamer outliers (%)	0.87	1.8
Clashscore	3.11	3.24
Average B-factor	23.93	20
macromolecules	22.66	18.32
ligands	25.95	21.99
solvent	33.39	30
No. TLS groups	1	1

^aData for the highest resolution shell are shown in parentheses

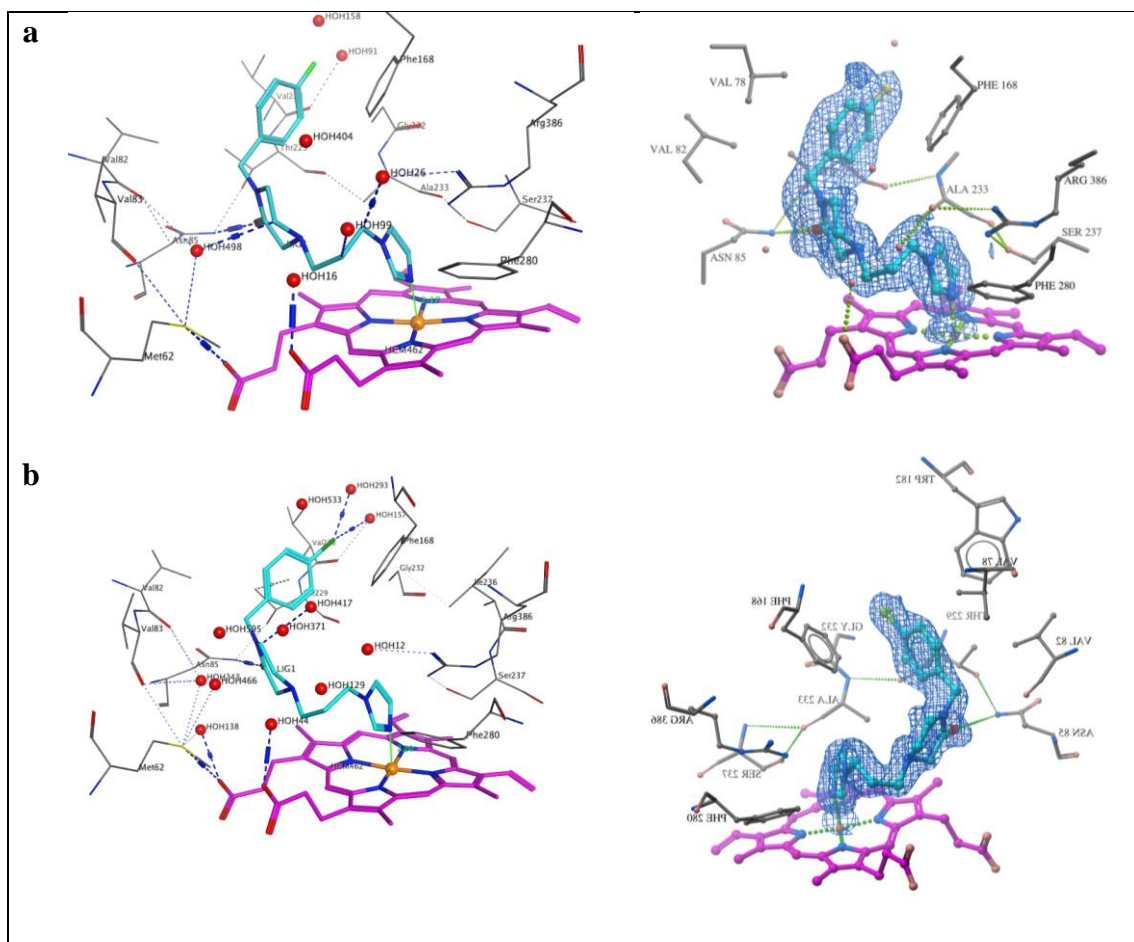


Figure 6. X-ray crystal structures and electron density maps of (a) **6a** and (b) **6b** binding to CYP121A1.

A 1.5 Å crystal structure of CYP121A1 in complex with compound **10a** was obtained. However, incomplete ligand occupancy prevented adequate refinement of the structure. Analysis of the ligand density of compound **10a** suggests that it likely acquires different binding orientations with two major conformations being rotated around the substituted piperazine central moiety of the ligand. In both orientations the imidazole groups are located pointing away from the heme towards the top of the active site cavity. In one orientation the 4-chloro group is situated 3.1 Å from the heme iron and is sandwiched between the active site residues Ser237 and Ala233 (Figure 7). In contrast, the same 4-chloro group in the second ligand orientation is 11.6 Å away from the iron and rotated 35.2 degrees from the former orientation with

respect to the heme iron (Figure 7). For this second orientation, the 2-4-dichlorobenzene ring stacks with the aromatic Phe168 residue that interacts with the one of the tyrosyls of the natural substrate cYY. The different orientations of compounds **10a** and the proximity of the halogen (4-Cl group) to the heme iron are in agreement with the UV-vis spectral data observed that reflect different binding modes and a degree of high-spin (HS) species present.

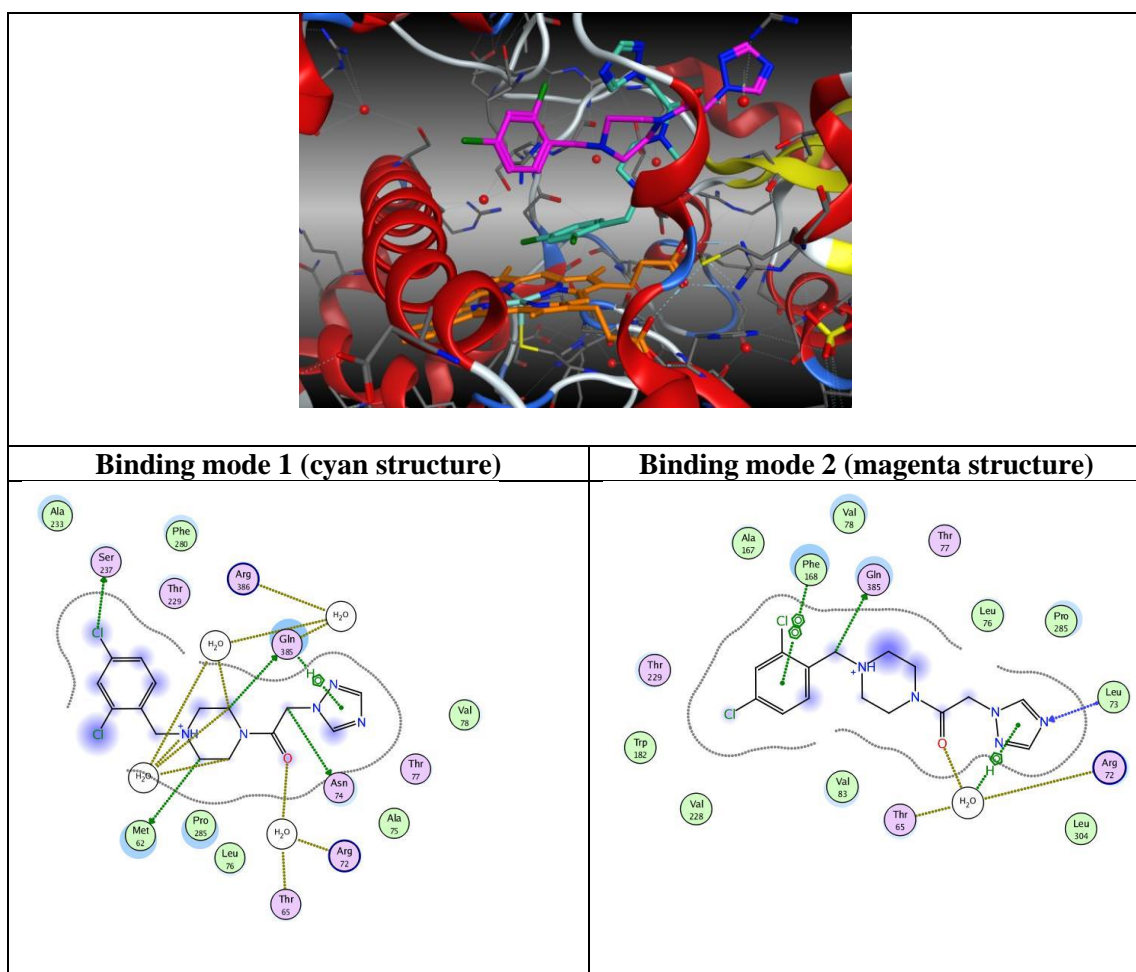


Figure 7. Multiple binding modes for compound **10a** in its complex with CYP121A1.

Flexible alignment of series C with cYY as shown in Table 4 (**17** (grey), natural substrate cYY (yellow)), indicated the overlap of the cYY tyrosyl groups with the two aromatic moieties. The cYY ketopiperazine ring is overlapped with the piperazine,

while the imidazole and triazole rings are placed in the same position of the cYY carbonyl group, but at a longer distance where they act as hydrogen bond acceptors. The score of alignment is shown in Table 4 with compound **17c** showing the best score (Table 4).

Table 4. Score of flexible alignment of series C compounds

Compound	R	X	Score (Kcal/mol)
17a	H	CH	-21.99
17b	H	N	-36.39
17c	OCH ₃	N	-38.30
17d	3,5-dimethoxy	CH	-19.44

From docking studies using MOE (Molecular Operating Environment) software²² it appeared that the orientation of the Series C piperazine derivatives (*S*- and *R*-enantiomers) in the CYP121A1 active site may allow the formation of a transition metal interaction directly between the nitrogen atom of the imidazole or triazole and the heme iron, as the distance was less than 3 Å. Hydrophobic interactions made by the series C compounds included those with Phe280, Ser237, Ala233, Pro285 and Thr77, which are key amino acids that interact with the natural substrate cYY (Figure 8). However, binding studies would suggest indirect binding to the heme via a water molecule might be the more likely interaction mode.

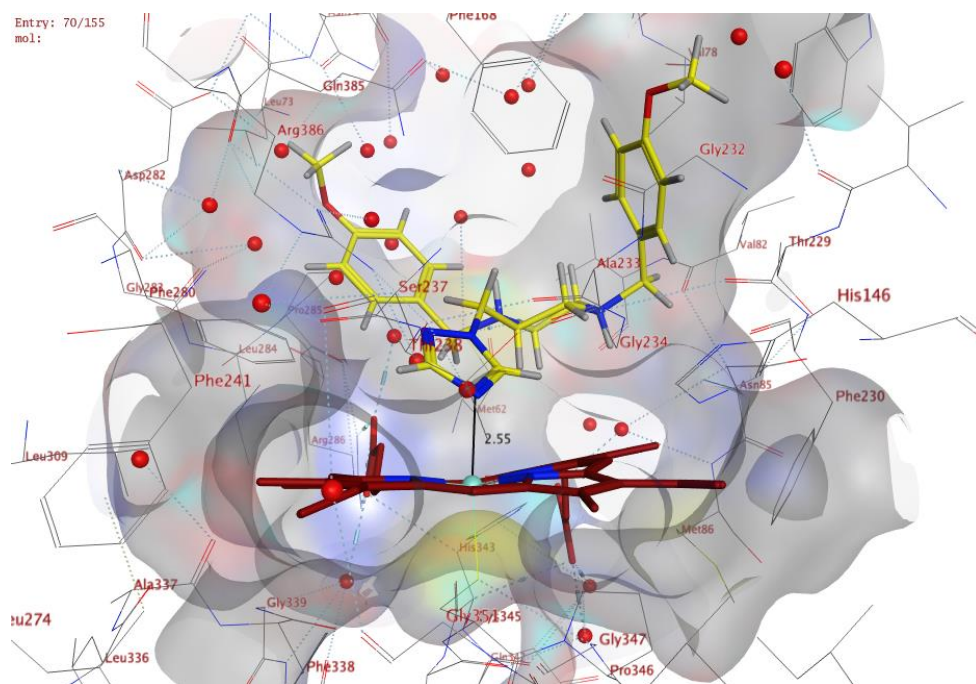


Figure 8. Docking of the Series C piperazine derivative (*S*)-**17c** into the CYP121A1 active site showing the distance (2.55 Å) between the triazole nitrogen and the haem iron.

3. Conclusions

A series of novel ligands were developed as potential inhibitors of the Mtb P450 enzyme CYP121A1 (Figure 3). These molecules are structural mimics of the natural cYY substrate, but to which a heme iron-coordinating imidazole or triazole group are appended in different positions on the scaffold, with other functional groups also introduced in place of the hydroxyl group(s) in cYY. For series A, crystallography would indicate a direct binding interaction with the haem iron. However, this does not translate to strong binding affinity. It could be that the structures are just locked in a ‘bound’ orientation that favors their structural solution, whereas in solution they are more mobile as indicated by the small spectral changes observed in the UV-Vis spectrum. In series B compound **10a** showed a distinct type I binding mode (Figure 5) further supported by a significant perturbation of the EPR spectrum with a 9-fold increase in the amount of HS ferric heme iron (Table 2, Figure 6). Further

development of series C molecules is warranted based on their inhibitory activity against Mtb (Table 1). While CYP121A1 optical binding assays do not show significant perturbation of the heme spectrum, this may be due to the series C inhibitors binding in an orientation that does not influence the heme axial coordination environment. However, at present we cannot conclude definitively that the activity against Mtb results from inhibition of CYP121A1. Binding affinity in the low μM range against CYP121A1 has been reported by Fonvielle *et al*⁹ for cYY derivatives and by Hudson *et al*^{23,24} for small fragment heterocyclic inhibitors. However, no inhibitory activity (i.e. MIC values) against Mtb has been reported, and so it is unknown whether the binding affinity would translate to a potent MIC value. Similarly, the antifungal azole fluconazole shows good CYP121A1 binding affinity, but no Mtb inhibitory activity²⁵ (although other azole drugs, e.g. econazole, do possess anti-Mtb activity).¹⁸ There are 20 different P450 isoforms encoded within the *M. tuberculosis* genome,²⁶ a number of which are considered important for pathogenicity and survival in the host, and these P450s could provide novel drug targets against pathogenic mycobacteria. The synthesis of CYP121A1 inhibitors is still in its infancy and, with the exact physiological role of this enzyme still to be determined, the development of selective inhibitors will be important for the analysis of CYP121A1 mechanism, as well as being potential leads for new antibiotics that target cytochrome P450 monooxygenase chemistry in Mtb.

4. Experimental

4.1 General Experimental

All chemicals, reagents and solvents were purchased from Sigma-Aldrich and Fisher Scientific companies and the required solvents were dried and stored over

4 Å molecular sieves under nitrogen. Flash column chromatography was performed with silica gel 60 (Merck 40–60 nm, 230–400 mesh) and TLC was performed on precoated silica gel plates (Merck Kiesegel 60 F₂₅₄) with visualization via UV light (254 nm) and / or vanillin stain. Melting points were determined on an electrothermal instrument (Gallenkamp) and are uncorrected. Compounds were visualized by irradiation with UV light at 250 nm and 366 nm. ¹H and ¹³C-NMR spectra were recorded on a Bruker Advance DPX500 spectrometer operating at 500 MHz and 125 MHz. Mass spectra (LRMS and HRMS) were determined under EI (Electron Impact) or CI (Chemical Ionization) conditions at the EPSRC National Mass Spectrometry Service Centre, University of Wales, Swansea, or at the Department of Chemistry, University of Wales, Cardiff. Microanalysis data were performed by Medac Ltd., Brunel Science Centre, Surrey. The chloroacetyl derivatives (**9**) imines (**12**) and diamines (**13**) were prepared as previously described.¹⁵⁻¹⁷

4.2 Chemistry

4.2.1. General method for the synthesis of 1-Boc- 4-(substituted)-3-oxopiperazine

(**3**)

To a solution of 1-Boc-3-oxopiperazine (**2**) (0.5 g, 2.49 mmol) in anhydrous DMF (10 mL) was added NaH (60% dispersion in mineral oil) (0.08 g, 3.7 mmol). The reaction was stirred at room temperature for 2 h then substituted benzyl chloride (**1**) (2.99 mmol) was added and the reaction heated at 70 °C overnight. The reaction mixture was cooled in an ice bath, quenched with water (5 mL) and then evaporated under reduced pressure. The product was extracted with ethyl acetate (100 mL) and washed with water (3 x 50 mL). The organic layer was dried (MgSO₄), evaporated under reduced pressure and the residue purified by flash chromatography using CH₂Cl₂:CH₃OH gradient elution unless stated otherwise.

4.2.1.1. *tert*-Butyl 4-(4-fluorobenzyl)-3-oxopiperazine-1-carboxylate (**3a**)¹³

Synthesised using 1-chloromethyl-4-fluorobenzene (0.43 g, 2.9 mmol). Yield: 63% as a white solid, m.p: 86-92 °C. ¹H-NMR (CDCl₃): δ 7.20 (m, 2H, Ar), 7.03 (m, 2H, Ar), 4.59 (s, 2H, CH₂), 4.10 (s, 2H, CH₂), 3.60 (t, J = 5.5 Hz, 2H, CH₂), 3.27 (t, J = 5.5 Hz, 2H, CH₂), 1.17 (s, 9H, *t*-Bu). ¹³C-NMR (CDCl₃): δ 165.8 (C=O, piperazine), 163.4, 161.4 (C-F), 153.8 (C=O), 132.1 (C), 132.05 (2 x CH, Ar), 115.7 (2 x CH, Ar), 80.9 (C, *t*-Bu), 49.3 (2 x CH₂), 45.6 (2 x CH₂), 28.6 (3 x CH₃, *t*-Bu).

4.2.1.2. *tert*-Butyl 4-(4-chlorobenzyl)-3-oxopiperazine-1-carboxylate (**3b**)

Synthesised according to the general procedure using 4-chlorobenzylchloride (0.48 g, 2.9 mmol) the residue was purified by flash chromatography using petroleum ether: EtOAc, the product was collected at 40:60 v/v. Yield: 41% as a white solid, m.p: 80-82 °C. ¹H-NMR (CDCl₃): δ 7.32 (d, J = 8.4 Hz, 2H, Ar), 7.22 (d, J = 8.4 Hz, 2H, Ar), 4.59 (s, 2H, CH₂), 4.16 (s, 2H, CH₂), 3.60 (t, J = 5.4 Hz, 2H, CH₂), 3.26 (t, J = 5.2 Hz, 2H, CH₂), 1.48 (s, 9H, *t*-Bu). ¹³C-NMR (CDCl₃): δ 164.8 (C=O, piperazine), 153.8 (C=O), 134.8 (C), 133.7 (C), 129.6 (2 x CH, Ar), 129.0 (2 x CH), 80.9 (C, *t*-Bu), 49.5 (2 x CH₂), 45.7 (2 x CH₂), 28.3 (3 x CH₃, *t*-Bu). Anal. Calcd for C₁₆H₂₁ClN₂O₃ (324.80): C, 59.17; H, 6.52; N, 8.62. Found: C, 59.15; H, 6.43; N, 8.38.

4.2.1.3. *tert*-Butyl 4-(4-methoxybenzyl)-3-oxopiperazine-1-carboxylate (**3c**)

Synthesised using 4-methoxybenzylchloride (0.46 g, 2.9 mmol). Yield: 74% as a white solid, m.p: 96-98 °C. ¹H-NMR (CDCl₃): δ 7.2 (d, J = 8.6 Hz, 2H, Ar), 6.87 (d, J = 8.5 Hz, 2H, Ar), 4.56 (s, 2H, CH₂), 4.14 (s, 2H, CH₂), 3.8 (s, 3H, CH₃), 3.57 (t, J = 5.4 Hz, 2H, CH₂), 3.24 (t, J = 5.4 Hz, 2H, CH₂), 1.40 (s, 9H, *t*-Bu). ¹³C-NMR (CDCl₃): δ 165.6 (C=O, piperazine), 162.5 (C), 153.8 (C=O), 129.7 (2 x CH, Ar), 128.6 (C), 114.1 (2 x CH, Ar), 80.7 (C, *t*-Bu), 55.3 (CH₃), 49.3 (2 x CH₂), 45.3 (2 x

CH), 28.3 (3 x CH₃, *t*-Bu). Anal. Calcd for C₁₇H₂₄N₂O₄ (320.38): C, 63.73; H, 7.55; N, 8.70. Found: C, 63.48; H, 7.60; N, 8.60.

4.2.1.4. *tert*-Butyl-4-(2,4-dichlorobenzyl)-3-oxopiperazine-1-carboxylate (**3d**)

Synthesised according to the general procedure using 2,4-dichloro-1-(chloromethyl)benzene (0.58 g, 2.9 mmol), the residue was purified by flash chromatography using petroleum ether: EtOAc, the product was collected at 40:60 v/v. Yield: 85 % as a cream solid, m.p: 98-106 °C. ¹H-NMR (CDCl₃): δ 7.42 (d, J = 1.7 Hz, 1H, Ar), 7.26 (m, 2H, Ar), 4.75 (s, 2H, CH₂), 4.15 (s, 2H, CH₂), 3.64 (t, J = 5.4 Hz, 2H, CH₂), 3.33 (t, J = 5.4 Hz, 2H, CH₂), 1.49 (s, 9H, *t*-Bu). ¹³C-NMR (CDCl₃): δ 166.1 (C=O, piperazine), 153.8 (C=O), 134.4 (C), 134.2 (C), 132.4 (C), 130.7 (CH, Ar), 129.5 (CH, Ar), 127.66 (CH, Ar), 81.0 (C, *t*-Bu), 46.3 (2 x CH₂), 46.9 (2 x CH₂), 28.3 (3x CH₃, *t*-Bu). Anal. Calcd for C₁₆H₂₀Cl₂N₂O₃ (359.25): C, 53.49; H, 5.61; N, 7.99. Found: C, 53.62; H, 5.59; N, 7.70.

4.2.2. General method for the synthesis of 1-(substituted)-piperazin-2-ones (**4**)

To the N-Boc-protected amine (**3**) (2 mmol) was added to a HCl solution (4M in dioxane, 33 mL). The reaction was stirred overnight at room temperature then 4M aqueous NaOH was added until alkaline. The solution was extracted with ethyl acetate (4 x 50 mL) then the organic layers combined, dried (MgSO₄) and evaporated under reduced pressure. The product was pure enough for use in the next step.

4.2.2.1. 1-(4-Fluorobenzyl)-piperazin-2-one (**4a**)

Synthesised according to the general procedure using *tert*-butyl 4-(4-fluorobenzyl)-3-oxopiperazine-1-carboxylate **3a** (0.47 g, 1.52 mmol). Yield: 74% as a pale yellow oil. ¹H-NMR (CDCl₃): δ 7.21 (m, 2H, Ar), 7.02 (m, 2H, Ar), 4.57 (s, 2H, CH₂), 3.50 (s, 2H, CH₂), 3.22 (t, J = 5.5 Hz, 2H, CH₂), 3.04 (t, J = 5.5 Hz, 2H, CH₂), 1.92 (br.s, 1H,

NH). ^{13}C -NMR (CDCl_3): δ 167.8 (C=O), 163.3 (C-F), 161.3 (C-F), 132.5 (C), 129.9 (2 x CH, Ar), 115.6 (2 x CH, Ar), 50.3 (CH_2), 49.2 (CH_2), 47.2 (CH_2), 43.2 (CH_2).

4.2.2.2. 1-(4-Chlorobenzyl)-piperazin-2-one (**4b**)

Synthesised according to the general procedure using 4-(4-chlorobenzyl)-3-oxo-piperazine-1-carboxylic acid *tert*-butyl ester **3b** (0.33 g, 1.02 mmol). Yield: 74% as a pale yellow solid, m.p: 49-50 °C. ^1H -NMR (CDCl_3): δ 7.29 (d, J = 6.9 Hz, 2H, Ar), 7.20 (d, J = 7.1 Hz, 2H, Ar), 4.56 (s, 2H, CH_2), 3.58 (s, 2H, CH_2), 3.21 (t, J = 5.2 Hz, 2H, CH_2), 3.03 (t, J = 5.2, 2H, CH_2), 1.97 (br.s, 1H, NH). ^{13}C -NMR (CDCl_3): δ 167.9 (C=O), 135.2 (C), 133.4 (C), 129.6 (2 x CH, Ar), 128.8 (2 x CH, Ar), 50.3 (CH_2), 49.3 (CH_2), 47.3 (CH_2), 43.2 (CH_2).

4.2.2.3. 1-(4-Methoxybenzyl)-piperazin-2-one (**4c**)

Synthesised according to the general procedure using 4-(4-methoxybenzyl)-3-oxo-piperazine-1-carboxylic acid *tert*-butyl ester **3c** (0.46 g, 2.08 mmol). Yield: 70% as yellow crystals, m.p: 60-64 °C. ^1H -NMR (CDCl_3): δ 7.20 (d, J = 8.7 Hz, 2H, Ar), 6.86 (d, J = 8.7 Hz, 2H, Ar), 4.54 (s, 2H, CH_2), 3.80 (s, 3H, CH_3), 3.58 (s, 2H, CH_2), 3.20 (t, J = 5.5 Hz, 2H, CH_2), 3.02 (t, J = 5.5 Hz, 2H, CH_2), 1.85 (s, 1H, NH). ^{13}C -NMR (CDCl_3): δ 167.7 (C=O), 159.1 (C), 129.6 (2 x CH, Ar), 129.4 (C), 114.0 (2 x CH, Ar), 55.3 (CH_3), 50.4 (CH_2), 49.2 (CH_2), 47.0 (CH_2), 43.2 (CH_2).

4.2.2.4. 1-(2,4-Dichlorobenzyl)-piperazin-2-one (**4d**)

Synthesised according to the general procedure using 4-(2,4-dichlorobenzyl)-3-oxo-piperazine-1-carboxylic acid *tert*-butyl ester **3d** (0.76 g, 2.1 mmol). Yield: 72% as an orange coloured solid, m.p: 96-102 °C. ^1H -NMR (CDCl_3): δ 7.39 (d, J = 1.95 Hz, 1H, Ar), 7.25 (m, 2H, Ar), 4.71 (s, 2H, CH_2), 3.57 (s, 2H, CH_2), 3.27 (t, J = 5.5 Hz, 2H, CH_2), 3.08 (t, J = 5.2 Hz, 2H, CH_2). ^{13}C -NMR (CDCl_3): δ 168.1 (C=O), 134.4 (C),

133.9 (C), 132.8 (C), 130.4 (CH, Ar), 129.3 (CH, Ar), 127.5 (CH, Ar), 50.3 (CH₂), 47.9 (CH₂), 46.7 (CH₂), 43.2 (CH₂).

4.2.3. General methods for synthesis of 4-(bromopropyl)-1-(4-substituted-benzyl)-piperazin-2-one (5)

Method 1: To a solution of 1-(4-substituted-benzyl)-piperazin-2-one **4** (1 eq) in anhydrous acetone (10 mL/1.5 mmol) were added K₂CO₃ (3 eq) and dibromopropane (4 eq). The reaction mixture was stirred at room temperature for 4 days. The reaction mixture was filtered and the filtrate was evaporated. The formed residue was extracted with CH₂Cl₂ (100 mL) and washed with water (50 mL). The organic layer was dried (MgSO₄), evaporated under reduced pressure and purified by flash chromatography using CH₂Cl₂:CH₃OH gradient elution.

Method 2: To a cooled (0 °C) solution of 1-(4-substituted-benzyl)-piperazin-2-one **4** (1 eq) in anhydrous acetone (10 mL /1.5 mmol) was added LiHMDS (1.2 eq) and the reaction stirred at 0 °C for 1 h. Dibromopropane (2 eq) was added to the mixture and the reaction stirred at room temperature for 48 h. The solvent was evaporated and the residue extracted with CH₂Cl₂ (100 mL), washed with 2M aqueous NaHCO₃ (50 mL) and water (50 mL). The organic layer was dried (MgSO₄), evaporated under reduced pressure and purified by flash chromatography using CH₂Cl₂:CH₃OH gradient elution.

4.2.3.1. 4-(3-Bromopropyl)-1-(4-fluorobenzyl)-piperazin-2-one (5a)

Synthesised according to method 2 using 1-(4-fluorobenzyl)-piperazin-2-one **4a** (0.21 g, 1.05 mmol). Yield: 75% as an orange liquid. ¹H-NMR (CDCl₃): δ 7.24 (m, 2H, Ar), 7.00 (m, 2H, Ar), 4.55 (s, 2H, CH₂), 3.46 (t, J = 6.4 Hz, 2H, CH₂), 3.22 (t, J = 5.9 Hz, 2H, CH₂), 3.21 (s, 2H, CH₂), 2.65 (t, J = 5.4 Hz, 2H, CH₂), 2.54 (t, J = 6.8 Hz, 2H, CH₂), 2.01 (m, 2H, CH₂). ¹³C-NMR (CDCl₃): δ 167.0 (C=O), 163.2, 132.3 (C-F),

129.9 (2 x CH-Ar) 119.0 (C), 115.4 (CH, Ar), 115.4 (CH, Ar), 57.3 (CH₂), 55.3 (CH₂), 49.9 (CH₂), 49.1 (CH₂), 45.9 (CH₂), 31.2 (CH₂), 29.7 (CH₂). [ES-HRMS] calculated for C₁₄H₁₈BrFN₂O: 330.0566 [M+H]⁺. Found: 330.0566 [M+H]⁺.

4.2.3.2. 4-(3-Bromopropyl)-1-(4-chlorobenzyl)-piperazin-2-one (**5b**)

Synthesised according to method 1 using 1-(4-chlorobenzyl)-piperazin-2-one **4b** (0.17 g, 0.76 mmol). Yield: 42% as a yellow oil. ¹H-NMR (CDCl₃): δ 7.29 (d, J = 8.45 Hz, 2H, Ar), 7.20 (d, J = 8.45 Hz, 2H, Ar), 4.55 (s, 2H, CH₂), 3.46 (t, J = 6.5 Hz, 2H, CH₂), 3.22 (s, 2H, CH₂), 3.21 (t, J = 5.5 Hz, 2H, CH₂), 2.65 (t, J = 5.5 Hz, 2H, CH₂), 2.55 (t, J = 6.8 Hz, 2H, CH₂), 2.01 (m, 2H, CH₂). ¹³C-NMR (CDCl₃): δ 166.9 (C=O), 135.1 (C), 133.4 (C), 128.8 (2 x CH, Ar), 129.6 (2 x CH, Ar), 57.3 (CH₂), 55.3 (CH₂), 49.9 (CH₂), 48.8 (CH₂), 46.0 (CH₂), 31.2 (CH₂), 29.7 (CH₂). [ES-HRMS] calculated for C₁₄H₁₈BrClN₂O: 344.0291 [M]⁺. Found: 344.0283 [M]⁺.

4.2.3.3. 4-(3-Bromopropyl)-1-(4-methoxybenzyl)-piperazin-2-one (**5c**)

Synthesised according to method 1 using 1-(4-methoxybenzyl)-piperazin-2-one **4c** (0.37 g, 1.67 mmol). The residue was purified by flash chromatography with EtOAc:CH₃OH: gradient elution. Yield: 69% as a colourless oil. ¹H-NMR (CDCl₃): δ 7.20 (d, J = 8.7 Hz, 2H, Ar), 6.87 (d, J = 8.7 Hz, 2H, Ar), 4.54 (s, 2H, CH₂), 3.81 (s, 3H, OCH₃), 3.81 (s, 2H, CH₂), 3.23 (m, 4H, 2 x CH₂), 2.66 (t, J = 5.5 Hz, 2H, CH₂), 2.56 (t, J = 6.8 Hz, 2H, CH₂), 2.03 (dt, J = 6.6, 13.2 Hz, 2H, CH₂). ¹³C-NMR (CDCl₃): δ 166.6 (C=O), 159.1 (C), 129.6 (2 x CH, Ar), 128.6 (C), 114.1 (2 x CH, Ar), 57.3 (CH₂), 55.4 (CH₂), 55.3 (OCH₃), 50.0 (CH₂), 48.9 (CH₂), 45.6 (CH₂), 31.2 (CH₂), 29.7 (CH₂). [ES-HRMS] calculated for C₁₅H₂₁BrN₂O₂: 340.0786 [M]⁺. Found: 340.0786 [M]⁺.

4.2.3.4. 4-(3-Bromopropyl)-1-(2,4-dichlorobenzyl)-piperazin-2-one (**5d**)

Synthesised according to method 1 using 1-(2,4-dichlorobenzyl)-piperazin-2-one **4d** (0.27 g, 1.04 mmol). Yield: 61% as a yellow viscous oil. ¹H-NMR (CDCl₃): δ 7.41 (t, J = 1.1 Hz, 1H, Ar), 7.25 (m, 2H, Ar), 4.71 (s, 2H, CH₂), 3.49 (t, J = 6.5 Hz, 2H, CH₂), 3.30 (t, J = 5.5 Hz, 2H, CH₂), 3.25 (s, 2H, CH₂), 2.72 (t, J = 5.5 Hz, 2H, CH₂), 2.59 (t, J = 6.8 Hz, 2H, CH₂), 2.05 (dt, J = 6.6, 13.3 Hz, 2H, CH₂). ¹³C-NMR (CDCl₃): δ 167.2 (C=O), 134.4 (C), 133.9 (C), 132.7 (C), 130.4 (CH, Ar), 129.4 (CH, Ar), 127.6 (CH, Ar), 57.4 (CH₂), 55.4 (CH₂), 50.0 (CH₂), 46.6 (CH₂), 46.4 (CH₂), 31.1 (CH₂), 29.7 (CH₂).

4.2.4. General methods for synthesis of 4-(3-imidazol-1-yl-propyl)-1-(substituted)-piperazin-2-one (6)

To a solution of NaH (2 eq) in dry DMF (10 mL/2 mmol of **5**), imidazole (2 eq) was added, the reaction was stirred for 1 h at 30 °C then cooled to room temperature. 4-(Bromoalkyl)-1-(4-substituted-benzyl)-piperazin-2-one (**5**) (1 eq) was added to the reaction mixture and left stirring overnight at 45 °C. Water (3 mL) was added to quench excess NaH and the reaction was evaporated under reduced pressure. Water (50 mL) was added to the formed residue and the product was extracted with ethyl acetate (3 x 50 mL). The organic layers were combined and washed with water (50 mL). The organic layer was then dried (MgSO₄), evaporated under reduced pressure and purified by preparative TLC, using EtOAc : CH₃OH 5:1 v/v as eluent.

4.2.4.1. 4-(3-(1H-imidazol-1-yl)propyl)-1-(4-fluorobenzyl)piperazin-2-one (6a)

Synthesised according to the general procedure using **5a** (0.15 g, 0.45 mmol) Yield: 48% as a yellow oil. ¹H-NMR (CDCl₃): δ 7.47 (s, 1H, imidazole), 7.24 (m, 2H, Ar), 7.06 (s, 1H, imidazole), 7.02 (m, 2H, Ar), 6.90 (s, 1H, imidazole), 4.5 (s, 2H, CH₂), 4.04 (t, J = 6.7 Hz, 2H, CH₂), 3.23 (t, J = 5.4 Hz, 2H, CH₂), 3.19 (s, 2H, CH₂), 2.61 (t, J = 5.4 Hz, 2H, CH₂), 2.34 (t, J = 6.6 Hz, 2H, CH₂), 1.94 (m, 2H, CH₂). ¹³C-NMR

(CDCl₃): δ 166.7 (C=O), 163.3 (C-F), 161.3 (C-F), 137.3 (CH, imidazole), 132.3 (C), 129.9 (2 x CH-Ar), 129.5 (CH, imidazole), 118.8 (CH, imidazole), 115.5 (2 x CH, Ar), 57.1 (CH₂), 53.6 (CH₂), 50.0 (CH₂), 48.8 (CH₂), 45.8 (CH₂), 44.2 (CH₂), 27.9 (CH₂). [ES-HRMS] calculated for C₁₇H₂₁FN₄O: 316.1699 [M+H]⁺. Found: 316.1694 [M+H]⁺.

4.2.4.2. 4-(3-(1H-imidazol-1-yl)propyl)-1-(4-chlorobenzyl)piperazin-2-one (**6b**)

Synthesised according to the general procedure using **5b** (0.11 g, 0.32 mmol). Yield: 22% as a yellow oil. ¹H-NMR (CDCl₃): δ 7.40 (s, 1H, imidazole), 7.32 (d, J = 7.5 Hz, 2H, Ar), 7.22 (d, J = 9.0 Hz, 2H, Ar), 7.07 (s, 1H, imidazole), 6.91 (s, 1H, imidazole), 5.31 (s, 2H, CH₂), 4.58 (s, 2H, CH₂), 4.04 (t, J = 7.0 Hz, 2H, CH₂), 3.24 (t, J = 6.0 Hz, 2H, CH₂), 2.61 (t, J = 5.5 Hz, 2H, CH₂), 2.34 (t, J = 7.0 Hz, 2H, CH₂), 1.94 (m, 2H, CH₂). ¹³C-NMR (CDCl₃): δ 166.7 (C=O), 135.0 (C), 133.5 (C), 129.7 (2 x CH, Ar), 129.6 (CH, imidazole), 129.0 (CH, imidazole), 128.9 (2 x CH, Ar), 118.5 (CH, imidazole), 57.1 (CH₂), 53.6 (CH₂), 50.0 (CH₂), 48.9 (CH₂), 45.9 (CH₂), 44.2 (CH₂), 27.9 (CH₂). [ES-HRMS] calculated for C₁₇H₂₁ClN₄O: 332.1404 [M+H]⁺. Found: 332.1410 [M+H]⁺.

4.2.4.3. 4-(3-(1H-imidazol-1-yl)propyl)-1-(4-methoxybenzyl)piperazin-2-one (**6c**)

Synthesised according to the general procedure using **5c** (0.33 g, 0.97 mmol). Yield: 57% as a yellow liquid. ¹H-NMR (DMSO-d₆): δ 7.46 (s, 1H, imidazole), 7.20 (d, J = 8.7 Hz, 2H, Ar), 7.06 (s, 1H, imidazole), 6.90 (s, 1H, imidazole), 6.87 (d, J = 8.7 Hz, 2H, Ar), 4.54 (s, 2H, CH₂), 4.03 (t, J = 6.7 Hz, 2H, CH₂), 3.8 (s, 3H, CH₃), 3.22 (t, J = 5.5 Hz, 2H, CH₂), 3.18 (s, 2H, CH₂), 2.5 (t, J = 5.4 Hz, CH₂), 2.32 (t, J = 6.7 Hz, 2H, CH₂), 1.93 (m, , 2H, CH₂). ¹³C-NMR (DMSO-d₆): δ 166.6 (C=O), 159.0 (C, Ar), 129.6 (2 x CH, Ar), 128.5 (C, Ar), 118.8 (CH-imidazole), 114.1 (2 x CH, Ar), 113.7 (CH, imidazole), 110.6 (CH, imidazole), 57.1 (CH₂), 55.3 (OCH₃), 53.6 (CH₂), 50.1

(CH₂), 48.9 (CH₂), 45.6 (CH₂), 44.2 (CH₂), 27.9 (CH₂). [ES-HRMS] calculated for C₁₈H₂₄N₄O₂: 328.1899 [M+H]⁺, Found: 328.1901 [M+H]⁺.

4.2.4.4. 4-(3-(1H-imidazol-1-yl)propyl)-1-(2,4-dichlorobenzyl)piperazin-2-one (**6d**)

Synthesised according to the general procedure using **5d** (0.27 g, 0.71 mmol). Yield: 51% as a yellow viscous oil. ¹H-NMR (CDCl₃): δ 7.07 (s, 1H, imidazole), 7.53 (s, 1H, imidazole), 7.40 (d, J = 1.2 Hz, 1H, Ar), 7.25 (m, 2H, Ar), 6.92 (s, 1H, imidazole), 4.71 (s, 2H, CH₂), 4.06 (t, J = 6.7 Hz, 2H, CH₂), 3.29 (t, J = 5.4 Hz, 2H, CH₂), 3.21 (br.s, 2H, CH₂), 2.65 (t, J = 5.4 Hz, 2H, CH₂), 2.36 (t, J = 6.7 Hz, 2H, CH₂), 1.96 (dt, J = 6.7, 13.4 Hz, 2H, CH₂). ¹³C-NMR (CDCl₃): δ 167.0 (C=O), 137.2 (CH, imidazole), 134.3 (C), 133.9 (C), 132.6 (C), 130.3 (CH Ar), 129.3 (CH, Ar), 129.0 (CH, imidazole), 127.5 (CH, Ar), 118.9 (CH, imidazole), 57.0 (CH₂), 53.5 (CH₂), 49.9 (CH₂), 46.5 (CH₂), 46.4 (CH₂), 44.3 (CH₂), 27.8 (CH₂). [ES-HRMS] calculated for C₁₇H₂₀Cl₂N₄O: 366.1014 [M+H]⁺. Found: 366.1021 [M+H]⁺.

4.2.5. General method for the synthesis of 2-imidazol or triazol-1-yl-1-[(substituted-benzyl)piperazin-1-yl]ethanone (**10**)

To a stirred suspension of potassium carbonate (4 eq) in dry CH₃CN (10 mL/5 mmol of **9**), imidazole or 1,2,4-triazole (4 eq) was added. The mixture was heated under reflux for 1 h at 45 °C and monitored using TLC system CH₃OH:EtOAc 1:4 v/v. The reaction was cooled to room temperature then the crude 1-(substituted-benzyl)piperazin-1-yl)-2-chloroethanone **9** (1eq) was added. The reaction was heated under reflux at 70 °C overnight. The solvent was evaporated, then water (30 mL) was added and then extracted with CH₂Cl₂ (3 x 30 mL). The organic layer was dried (MgSO₄), evaporated under reduced pressure and purified by preparative TLC using CH₃OH:EtOAc 1:4 v/v.

4.2.5.1. *1-(4-(2,4-Dichlorobenzyl)piperazin-1-yl)-2-(1H-1,2,4-triazol-1-yl)ethanone (10a)*

Synthesized using 2-chloro-1-[4-(2,4-dichlorobenzyl)-piperazin-1-yl]-ethanone (0.6 g, 1.8 mmol). Yield: 32% as a pale yellow solid, m.p: 70-74 ° C. ¹H-NMR (CDCl₃): δ 8.25 (s, 1H, triazole), 7.97 (s, 1H, triazole), 7.42 (d, J = 2.1 Hz, 1H, Ar), 7.40 (d, J = 2.1 Hz, 1H, Ar), 7.25 (dd, J = 2.1, 8.3 Hz, 1H, Ar), 5.06 (s, 2H, CH₂CO), 3.68 (app.s, 2H, CH₂-piperazine), 3.64 (s, 2H, PhCH₂), 3.58 (app.s, 2H, CH₂-piperazine), 2.55 (m, 4H, 2 x CH₂- piperazine). ¹³C-NMR (CDCl₃): δ 163.6 (C=O), 151.7 (CH, triazole), 144.7 (CH, triazole), 135.1 (2 x C), 133.8 (C), 131.6 (CH, Ar), 129.4 (CH, Ar), 127.1 (CH, Ar), 58.4 (CH₂), 52.7 (CH₂), 52.3 (CH₂), 50.4 (CH₂), 45.3 (CH₂), 42.3 (CH₂). [APCI-HRMS] calculated for C₁₅H₁₇C₁₂N₅: 354.0888 [M+H]⁺. Found: 354.0890 [M+H]⁺.

4.2.5.2. *1-(4-(4-Fluorobenzyl)piperazin-1-yl)-2-(1H-1,2,4-triazol-1-yl)ethanone (10b)*

Synthesized using 2-chloro-1-[4-(4-fluorobenzyl)piperazin-1-yl]ethanone (0.2 g, 0.7 mmol). Yield: 35% as a yellow solid, m.p: 116-120 °C. ¹H-NMR (CDCl₃): δ 8.25 (s, 1H, triazole), 7.95 (s, 1H, triazole), 7.30 (m, 2H, Ar), 7.02 (m, 2H, Ar), 5.06 (s, 2H, CH₂CO), 3.67 (t, J = 4.5 Hz, 2H, CH₂-piperazine), 4.56 (t, J = 4.7 Hz, 2H, CH₂-piperazine), 3.52 (s, 2H, PhCH₂), 2.47 (m, 4H, 2 x CH₂-piperazine). ¹³C-NMR (CDCl₃): δ 163.6 (C=O), 163.2, 161.3 (C-F), 151.7 (CH, triazole), 144.8 (CH, triazole), 130.7 (CH, Ar), 130.7 (CH, Ar), 115.4 (CH, Ar), 115.2 (CH, Ar), 62.1 (CH₂), 52.6 (CH₂), 52.2 (CH₂), 50.4 (CH₂), 45.2 (CH₂), 42.2 (CH₂). [APCI- HRMS] calculated for C₁₅H₁₈FN₅O: 304.1574 [M+H]⁺. Found: 304.1561 [M+H]⁺.

4.2.5.3. *1-(4-(4-Fluorobenzyl)piperazin-1-yl)-2-(1H-imidazol-1-yl)ethanone (10c)*

Synthesized using 2-chloro-1-[4-(4-fluorobenzyl)-piperazin-1-yl]-ethanone (0.2 g, 0.7 mmol). Yield: 36% as a yellow oil. ¹H-NMR (CDCl₃): δ 7.51(s, 1H, imidazole), 7.28

(m, 2H, Ar), 7.08 (s, 1H, imidazole), 7.03 (m, 2H, Ar), 6.9 (s, 1H, imidazole), 4.77 (s, 2H, CH₂CO), 3.64 (br.s, 2H, CH₂-piperazine), 3.57 (s, 2H, PhCH₂), 3.45 (br.s, 2H, CH₂-piperazine), 2.43 (br.s, 4H, 2 x CH₂-piperazine). ¹³C-NMR (CDCl₃): δ 164.5 (C=O), 163.1, 161.2 (C-F), 138.0 (CH, imidazole), 133.1 (C), 130.6 (2 x CH, Ar), 129.1 (CH, imidazole), 120.2 (CH, imidazole), 115.2 (CH, Ar), 115.1 (CH, Ar), 61.97 (CH₂), 52.6 (CH₂), 52.4 (CH₂), 48.0 (CH₂), 45.1 (CH₂), 42.3 (CH₂). [APCI-HRMS] calculated for C₁₆H₁₉FN₄O: 303.1621[M+H]⁺. Found: 303.1608 [M+H]⁺.

4.2.6. General procedure for the synthesis of ethyl 1,4-bis(substituted benzyl)piperazine-2-carboxylate (14)

2,3-Dibromopropionic acid ethyl ester (1.04 eq) was added dropwise to a solution of diamine **13** (1 eq) in hot dry toluene at 80 °C (70 mL/24 mmol of **13**) and triethylamine (2.5 eq). The reaction mixture was refluxed overnight then the reaction was cooled, washed with saturated aqueous NaHCO₃ (3 x 25 mL) and brine (2 x 25 mL). The organic layer was dried (MgSO₄), concentrated under reduced pressure and purified by flash chromatography gradient elution with CH₂Cl₂:CH₃OH. The pure product appeared at 1-2 % methanol, unless otherwise indicated.

4.2.6.1. Ethyl 1,4-dibenzylpiperazine-2-carboxylate (14a)²⁷

Synthesised according to the general procedure using *N,N'*-dibenzylethylenediamine **13a** (3.9 g, 16.33 mmol). Yield: 54% as a yellow oil. ¹H-NMR (CDCl₃): δ 7.33 (m, 8H, Ar), 7.28 (m, 2H, Ar), 4.21 (q, J = 3.5 Hz, 2H, CH₂CH₃), 3.96 (d, J = 13.3 Hz, 1H, CH₂Ph), 3.66 (m, 1H, CH₂Ph), 3.60 (d, J = 13.2 Hz, 1H, CH₂Ph), 3.49 (d, J = 13.2 Hz, 1H, CH₂Ph), 3.37 (m, 1H, CH-piperazine), 3.13 (m, 1H, piperazine), 2.86 (m, 1H, piperazine), 2.66 (d, J = 9.1 Hz, 1H, piperazine), 2.5 (m, 3H, piperazine), 1.32 (t, J = 7.1 Hz, 3H, CH₂CH₃). ¹³C-NMR (CDCl₃): δ 172.1 (C, C=O), 138.3 (C, Ar), 138.0 (C,

Ar), 129.0 (2 x CH, Ar), 128.8 (2 x CH, Ar), 128.6 (2 x CH, Ar), 128.5 (2 x CH, Ar), 127.5 (2 x CH, Ar), 62.8 (CH), 62.7 (CH₂), 60.4 (CH₂), 59.7 (CH₂), 55.5 (CH₂), 53.1 (CH₂), 48.6 (CH₂), 14.3 (CH₃).

4.2.6.2. Ethyl 1,4-bis(4-methoxybenzyl)piperazine-2-carboxylate (**14b**)

Synthesised according to the general procedure using *N,N'*-bis(4-methoxybenzyl)ethane-1,2-diamine **13b** (2 g, 6.6 mmol). Yield: 73% as an orange oil. ¹H-NMR (CDCl₃): δ 7.25 (d, J = 9.0 Hz, 2H, Ar), 7.21 (d, J = 7.5 Hz, 2H, Ar), 6.85 (m, 4H, Ar), 4.19 (q, J = 7.1 Hz, 2H, CH₂CH₃), 3.88 (d, J = 13.1 Hz, 1H, CH₂Ph), 3.78 (s, 6H, 2 x OCH₃), 3.51 (d, J = 13.0 Hz, 2H, CH₂Ph), 3.68 (d, J = 13.0 Hz, 1H, CH₂Ph), 3.29 (m, 1H, piperazine), 3.05 (m, 1H, piperazine), 2.69 (s, 1H, piperazine), 2.63 (s, 1H, piperazine), 2.48 (m, 2H, piperazine), 2.39 (m, 1H, piperazine), 1.26 (t, J = 7.1, 3H, CH₂CH₃). ¹³C-NMR (CDCl₃): δ 172.0 (C=O), 158.8 (C, 2 x C-OCH₃), 130.5 (2 x CH, Ar), 130.3 (2 x CH, Ar), 113.8 (4 x CH, Ar), 62.7 (CH), 61.9 (CH₂), 60.6 (CH₂), 58.9 (CH₂), 55.3 (2 x OCH₃), 55.2 (CH₂), 55.1 (CH₂), 52.7 (CH₂), 14.3 (CH₃). [ES-HRMS] calculated for C₂₃H₃₁N₂O₄: 399.2284 [M+H]⁺. Found: 399.2270 [M+H]⁺.

4.2.6.3. Ethyl 1,4-bis(3,5-dimethoxybenzyl)piperazine-2-carboxylate (**14c**)

Synthesised according to the general procedure using *N,N'*-bis(3,5-dimethoxybenzyl)ethane-1,2-diamine **13c** (1.5 g, 4.1 mmol). Yield: 68% as an orange solid, m.p. 58-60 °C. ¹H-NMR (CDCl₃): δ 6.53 (d, J = 2.1 Hz, 2H, Ar), 6.49 (d, J = 2.1 Hz, 2H, Ar), 6.37 (m, 2H, Ar), 4.20 (q, J = 7.1 Hz, 2H, CH₂CH₃), 3.88 (d, J = 13.5 Hz, 1H, PhCH₂), 3.797 (s, 6H, 2 x OCH₃), 3.791 (s, 6H, 2 x OCH₃), 3.61 (m, 1H, CH-piperazine), 3.52 (d, J = 13.5 Hz, 1H, CH₂Ph), 3.37 (d, J = 13.6 Hz, 2H, CH₂Ph), 3.15 (m, 1H, piperazine), 2.82 (m, 1H, piperazine), 2.59 (m, 2H, piperazine), 2.47 (m, 2H, piperazine), 1.25 (t, J = 7.1 Hz, 3H, CH₂CH₃). ¹³C-NMR (CDCl₃): δ 172.1 (C, C=O),

160.8 (4 x C, C-OCH₃), 140.8 (C, Ar), 140.6 (C, Ar), 106.8 (4 x CH, Ar), 99.1 (CH, Ar), 99.0 (CH, Ar), 62.7 (CH₂), 62.4 (CH), 60.3 (CH₂), 59.6 (CH₂), 55.5 (CH₂), 55.3 (4 x OCH₃), 53.2 (CH₂), 48.5 (CH₂), 14.2 (CH₃). [AP-HRMS] calculated for C₂₅H₃₅N₂O₆: 459.2495 [M+H]⁺. Found: 459.2475 [M+H]⁺.

4.2.7. General procedure for the synthesis of [1,4-bis(substituted benzyl)piperazin-2-yl]methanol (15)

A suspension of LiAlH₄ (4 eq, 1M in Et₂O) was diluted with dry Et₂O (15 mL/11 mmol LiAlH₄) then added to a solution of 1,4-bis(substituted-benzyl)piperazine-2-carboxylic acid ethyl ester **14** (1 eq) in dry Et₂O (20 mL/6 mmol of **14**) slowly over 1 h at 0 °C. The reaction was stirred overnight at room temperature, cooled to 0 °C and treated carefully with saturated aqueous NaHCO₃ until cessation of effervescence. The solution was extracted with ethyl acetate (3 x 50 mL), the organic layer was dried (MgSO₄), concentrated under reduced and purified by flash chromatography using gradient elution CH₂Cl₂:CH₃OH, and the product appeared at 2% methanol.

4.2.7.1. 1,4-Dibenzylpiperazin-2-yl-methanol (15a)²⁸

Synthesised according to the general procedure using 1,4-dibenzylpiperazine-2-carboxylic acid ethyl ester **14a** (3.1 g, 9.1 mmol). Yield: 92% as a yellow oil. ¹H-NMR (CDCl₃): δ 7.35 (m, 8H, Ar), 7.28 (m, 2H, Ar), 4.05 (dd, J = 2.5 Hz, 10.9 Hz, 2H, CH₂), 3.65 (dd, J = 2.6, 11.2 Hz, 1H), 3.43 (s, 2H, CH₂), 3.50 (d, J = 13.5 Hz, 1H), 2.97 (m, 1H, piperazine), 2.76 (dd, 2.6, 10.8 Hz, 1H, piperazine), 2.68 (m, 1H, piperazine), 2.58 (m, 2H, piperazine), 2.48 (m, 1H, piperazine), 2.40 (m, 1H, piperazine). ¹³C-NMR (CDCl₃): δ 138.5 (C, Ar), 137.6 (C, Ar), 129.2 (2 x CH, Ar), 128.7 (2 x CH, Ar), 128.4 (2 x CH, Ar), 127.5 (2 x CH, Ar), 127.4 (2 x CH, Ar), 63.0 (CH₂), 62.1 (CH₂), 58.5 (CH), 58.1 (CH₂), 56.0 (CH₂), 53.0 (CH₂), 50.0 (CH₂).

4.2.7.2. 1,4-Bis(4-methoxybenzyl)piperazin-2-yl]methanol (15b)²⁹

Synthesised according to the general procedure using 1,4-bis(4-methoxybenzyl)piperazine-2-carboxylic acid ethyl ester **14b** (1.9 mL, 4.7 mmol). Yield: 62% as a beige solid, m.p: 94-96 °C. ¹H-NMR (CDCl₃): δ 7.22 (t, J = 8.0 Hz, 2H, Ar), 6.85 (dd, J = 2.0, 9.0 Hz, 2H, Ar), 3.98 (m, 2H, CH₂), 3.77 (s, 6H, 2 x OCH₃), 3.75 (s, obscured 1H, CH₂), 3.61 (m, 1H, CH₂), 3.37 (m, 2H, CH₂), 2.92 (m, 1H, piperazine), 2.71-2.33 (m, 6H, piperazine). ¹³C-NMR (CDCl₃): δ 158.8 (C, C-OCH₃), 158.7 (C, C-OCH₃), 130.3 (2 x CH, Ar), 130.2 (C, Ar), 129.9 (2 x CH, Ar), 129.7 (C, Ar), 114.0 (CH, Ar), 62.8 (CH₂), 62.5 (CH₂), 58.9 (CH), 57.8 (CH₂), 56.1 (CH₂), 55.2 (CH₃), 52.4 (CH₂), 49.9 (CH₂).

4.2.7.3. [1,4-Bis(3,5-dimethoxybenzyl)piperazin-2-yl]methanol (**15c**)

Synthesised according to the general procedure using 1,4-bis(3,5-dimethoxybenzyl)piperazine-2-carboxylic acid ethyl ester **14c** (1.17g, 2.5 mmol). Yield: 50% as a yellow oil. ¹H-NMR (CDCl₃): δ 6.41 (d, J = 2.2 Hz, 2H, Ar), 6.39 (d, J = 2.2 Hz, 2H, Ar), 6.26 (m, 2 x CH, Ar), 3.90 (dd, J = 3.3, 11.3 Hz, 1H), 3.82 (d, J = 13.1 Hz, 1H), 3.68 (s, 12H, 4 x OCH₃), 3.35 (d, J = 13.5 Hz, 1H), 3.35 (m, 3H), 2.89 (m, 1H, piperazine), 2.58 (m, 2H, piperazine), 2.60 (m, 1H, piperazine), 2.41 (m, 2H, piperazine), 2.33 (m, 1H, CH-piperazine). ¹³C-NMR (CDCl₃): δ 160.9 (2 x C), 160.8 (2 x C), 141.0 (C), 140.0 (C), 107.2 (2 x CH, Ar), 106.9 (2 x CH, Ar), 99.3 (CH, Ar), 99.0 (CH, Ar), 63.2 (CH₂), 62.1 (CH₂), 58.9 (CH), 58.2 (CH₂), 58.0 (CH₂), 55.3 (4 x OCH₃), 52.4 (CH₂), 49.89 (CH₂). [AP-HRMS] calculated for C₂₃H₃₃N₂O₅: 417.2389 [M+H]⁺. Found: 417.2394 [M+H]⁺.

4.2.8. General procedure for the synthesis of 1,4-Bis(substituted-benzyl)-2-chloromethylpiperazine (**16**)

To 1,4-bis(substituted benzyl)piperazin-2-yl]-methanol **15** (1 eq) in dry toluene (20 mL/1 mmol of **15**) was added SOCl₂ (2 eq) slowly while cooling in an ice bath. The

reaction mixture was refluxed overnight at 80 °C then cooled to room temperature and washed with saturated aqueous NaHCO₃ (3 x 30 mL), brine (2 x 20 mL) and water (2 x 20 mL). The organic layer was dried (MgSO₄) and concentrated under reduced pressure.

4.2.8.1. 1,4-Dibenzyl-2-chloromethylpiperazine (**16a**)

Synthesised according to the general procedure using (1,4-dibenzylpiperazin-2-yl)methanol **15a** (2 g, 6.7 mmol). The product was pure enough to proceed to the next step. Yield: 76% as a yellowish orange oil. ¹H-NMR (CDCl₃): δ 7.39 (m, 8H, Ar), 7.31 (m, 2H, Ar), 3.96 (m, 2H, CH₂), 3.76 (dd, J = 2.8, 11.1 Hz, 1H), 3.59 (d, J = 6 Hz, 2H, CH₂), 3.56 (d, J = 13.3 Hz, 1H), 2.92 (m, 1H, piperazine), 2.77 (m, 1H, piperazine), 2.70 (d, J = 4.2 Hz, 2H, piperazine), 2.52 (m, 1H, piperazine), 2.44 (d, J = 7.4 Hz, 2H, piperazine). ¹³C NMR (CDCl₃): δ 138.6 (C), 138.1 (C), 129.4 (2 x CH, Ar), 129.3 (2 x CH, Ar), 128.7 (2 x CH, Ar), 128.5 (2 x CH, Ar), 127.3 (2 x CH, Ar), 62.9 (CH₂), 62.0 (CH), 60.4 (CH₂), 58.2 (CH₂), 55.8 (CH₂), 49.1 (CH₂), 42.6 (CH₂).

4.2.8.2. 2-Chloromethyl-1,4-bis(4-methoxybenzyl)piperazine (**16b**)

Synthesised according to the general procedure using 1,4-bis(4-methoxybenzyl)piperazin-2-yl]methanol **15b** (1 g, 2.8 mmol). Obtained as a white crystalline solid after recrystallisation from methanol. Yield: 31%, m.p. 76-82 °C. ¹H-NMR (CDCl₃): δ 7.26 (m, 4H, Ar), 7.87 (m, 4H, Ar), 3.91 (m, 2H, CH₂), 3.82 (s, 3H, OCH₃), 3.81 (s, 3H, OCH₃), 3.70 (dd, J = 2.6, 11.2 Hz, 1H), 3.50 (m, 2H, CH₂), 3.42 (d, J = 13.1 Hz, 1H), 2.87 (m, 1H, piperazine), 2.73 (m, 1H, piperazine), 2.63 (m, 2H, piperazine), 2.50 (m, 1H, piperazine), 2.4 (d, J = 6.4 Hz, 2H, piperazine). ¹³C-NMR (CDCl₃): δ 158.9 (C), 158.8 (C), 130.4 (2 x CH, Ar), 130.2 (2 x C), 130.0 (2 x CH, Ar), 113.9 (4 x CH, Ar), 62.1 (CH₂), 59.9 (CH), 57.4 (CH₂), 55.3 (CH₃), 55.1 (CH₂),

52.5 (CH₂), 48.9 (CH₂), 42.7 (CH₂). [AP-HRMS] calculated for C₂₁H₂₈ClN₂O₂: 375.1839 [M+H]⁺. Found: 375.1831 [M+H]⁺.

4.2.9. General procedure for the synthesis of 1,4-bis(substituted-benzyl)-2-imidazol-1-ylmethyl-piperazine and 1,4-bis(substituted-benzyl)-2-[1,2,4]triazol-1-ylmethyl-piperazine (17).

To a solution of imidazole or triazole (4 eq) in dry DMF (5 mL/2.5 mmol of starting material) was added NaH (60% dispersion in mineral oil, 4 eq). After refluxing the mixture for 1 h at 40 °C, a solution of 1,4-bis(substituted-benzyl)-2-chloromethyl-piperazine **16** (1 eq) in dry DMF (5 mL/2.5 mmol of **16**) and KI (1.08 eq) was added to the mixture and refluxed overnight at 60 °C. The reaction was cooled, diluted with EtOAc (100 mL) and washed with brine (2 x 10 mL) and water (2 x 10 mL), the organic layer was dried (MgSO₄), evaporated and the resulting residue was further purified.

4.2.9.1. 1,4-Dibenzyl-2-imidazol-1-yl-methylpiperazine (17a)

Synthesised according to the general procedure using 1,4-dibenzyl-2-chloromethylpiperazine **16a** (0.8 g, 2.5 mmol), imidazole (0.66 g, 10 mmol). The product was purified by flash chromatography using gradient elution of CH₂Cl₂:CH₃OH, the product appeared at 2% methanol. Yield: 63% as a yellowish orange semi-solid. ¹H-NMR (CDCl₃): δ 7.32 (m, 8H, Ar), 7.25 (s, 1H, imidazole), 6.96 (s, 1H, imidazole), 6.64 (s, 1H, imidazole), 4.30 (m, 1H), 4.15 (dd, J = 4.0, 13.7 Hz, 1H), 3.89 (d, J = 13.4 Hz, 1H), 3.67 (dd, J = 5.0, 18.5 Hz, 1H), 3.53 (d, J = 12.8 Hz, 1H), 3.37 (d, J = 12.8 Hz, 1H), 2.87 (m, 2H, piperazine), 2.56 (m, 2H, piperazine), 2.41 (m, 1H, piperazine), 2.3 (d, J = 3.4 Hz, 2H, piperazine). ¹³C-NMR (CDCl₃): δ 138.3 (C, Ar), 138.3 (C, Ar), 137.6 (CH, imidazole), 129.8 (2 x CH, Ar), 129.0 (CH, imidazole), 128.6 (2 x CH, Ar), 128.5 (2 x CH, Ar), 128.4 (2 x CH, Ar),

127.4 (2 x CH, Ar), 119.5 (CH, imidazole), 63.3 (2 x CH₂), 58.5 (CH), 58.3 (2 x CH₂), 52.5 (2 x CH₂). [AP-HRMS] calculated for C₂₂H₂₇N₄: 347.2236 [M+H]⁺. Found: 347.2222 [M+H]⁺.

4.2.9.2. 1,4-Dibenzyl-2-[1,2,4]triazol-1-yl-methylpiperazine (**17b**)

Synthesised according to the general procedure using 1,4-dibenzyl-2-chloromethylpiperazine **16a** (0.8 g, 2.5 mmol), triazole (0.66 g, 10 mmol). The product was purified by flash chromatography using gradient elution of CH₂Cl₂:CH₃OH, the product appeared at 2% methanol. Yield: 57% as a yellowish orange oil. ¹H-NMR (CDCl₃): δ 7.88 (s, 1H, triazole), 7.81 (s, 1H, triazole), 7.31 (m, 10H, Ar), 4.54 (s, 1H), 4.47 (dd, J = 4.6, 13.6 Hz, 1H), 3.85 (d, J = 13.4 Hz, 1H), 3.75 (d, J = 13.4 Hz, 1H), 3.58 (d, J = 11.0 Hz, 1H), 3.40 (d, J = 12.2 Hz, 1H), 3.18 (m, 1H, piperazine), 2.85 (s, 1H, piperazine), 2.42 (s, 2H, piperazine), 2.57 (s, 2H, piperazine), 2.32 (d, J = 9.1 Hz, 1H, piperazine). ¹³C-NMR (CDCl₃): δ 151.9 (CH, triazole), 143.8 (CH, triazole), 138.6 (2 x C), 129.3 (2 x CH, Ar), 128.8 (2 x CH, Ar), 128.6 (2 x CH, Ar), 128.4 (2 x CH, Ar), 127.3 (2 x CH, Ar), 62.8 (2 x CH₂), 58.3 (2 x CH₂), 57.9 (CH), 52.3 (2 x CH₂). [ES-HRMS] calculated for C₂₁H₂₆N₅: 348.4646 [M+H]⁺. Found: 348.4638 [M+H]⁺.

4.2.9.3. 1,4-Bis(4-methoxybenzyl)-2-[1,2,4]triazol-1-ylmethyl-piperazine (**17c**)

Synthesised according to the general procedure using 2-chloromethyl-1,4-bis(4-methoxybenzyl)piperazine **16b** (0.31 g, 0.8 mmol), triazole (0.21 g, 3.2 mmol). The product was purified by preparative TLC using CH₂Cl₂: CH₃OH 95:5 v/v as eluent. Yield: 36% as a yellowish orange oil. ¹H-NMR (CDCl₃): δ 7.88 (s, 2H, triazole), 7.20 (d, J = 8.0 Hz, 2H, Ar), 7.18 (d, J = 8.6 Hz, 2H, Ar), 6.86 (m, 4H, Ar), 4.49 (d, J = 4.7 Hz, 1H), 4.46 (dd, J = 4.7, 13.7 Hz, 1H), 3.82 (s, 3H, CH₃), 3.80 (s, 3H, CH₃), 3.78 (obscured d, 1H), 3.66 (d, J = 5.0 Hz, 1H), 3.49 (d, J = 11.9 Hz, 1H), 3.35 (d, J = 12.7

Hz, 1H), 3.17 (m, 1H, piperazine), 2.85 (m, 1H, piperazine), 2.52 (d, J = 11.5 Hz, 2H, piperazine), 2.38 (d, J = 8.8 Hz, 2H, piperazine), 2.28 (dd, J = 3.7, 11.4 Hz, 1H, piperazine). ¹³C-NMR (CDCl₃): δ 159.0 (C, C-OCH₃), 158.8 (C, C-OCH₃), 151.8 (CH, triazole), 143.8 (CH, triazole), 132.0 (CH, Ar), 129.9 (2 x CH, Ar), 114.1 (4 x CH, Ar), 62.2 (2 x CH₂), 57.8 (CH), 57.6 (2 x CH₂), 55.3 (CH₃), 55.3 (CH₃), 52.0 (2 x CH₂). [ES-HRMS] calculated for C₂₃H₃₀N₅O₂: 408.2394 [M+H]⁺. Found: 408.2385 [M+H]⁺.

4.2.9.4. 1,4-Bis(3,5-dimethoxybenzyl)2-imidazole-1-ylmethyl-piperazine (**17d**)

To a solution of [1,4-bis(3,5-dimethoxybenzyl)-piperazin-2-yl]-methanol **15c** (0.25 g, 0.6 mmol) in dry CH₂Cl₂ (30 mL) was added methanesulfonylchloride (0.05 mL, 0.69 mmol) and triethylamine (0.16 mL, 1.18 mmol) at 0 °C. The resulting mixture was stirred at room for 2 h. After quenching the reaction with water (20 mL), the organic phase was washed with water (2 x 20 mL), dried (MgSO₄) and evaporated under vacuum. The resulting methane sulfonate derivative was added to a solution of imidazole sodium salt (prepared from imidazole (0.12 g, 1.7 mmol) and NaH 60% dispersion in mineral oil (0.04 g, 1.7 mmol) in dry toluene (20 mL), previously refluxed at 40 °C for 1h) and the reaction mixture refluxed overnight at 115 °C. The reaction was cooled to room temperature and washed with water (5 x 25 mL). The organic layer was separated, dried (MgSO₄), evaporated under vacuum and purified by preparative TLC using CH₂Cl₂:CH₃OH 98:2 v/v. Yield: 14% as an oily yellow orange solid. ¹H-NMR (CDCl₃): δ 7.25 (s, 1H, imidazole), 6.88 (s, 1H, imidazole), 6.31 (s, 1H, imidazole), 6.42 (m, 4H, Ar), 6.31 (m, 2H, Ar), 4.21 (m, 1H), 4.11 (dd, J = 4.3, 13.8 Hz, 1H), 3.71 (s, 6H, 2 x OCH₃), 3.70 (s, 6H, 2 x OCH₃), 3.69 (d, J = 10.3 Hz, 1H), 3.38 (m, 1H), 3.25 (d, J = 13.0 Hz, 2H), 2.81 (m, 1H, piperazine), 2.68 (m, 1H, piperazine), 2.55 (m, 1H, piperazine), 2.48 (m, 2H, piperazine), 2.35 (m, 1H,

piperazine), 2.23 (m, 1H, piperazine). ^{13}C NMR (CDCl_3): δ 160.9 (2 x C), 160.85 (2 x C), 140.9 (C), 140.6 (C), 137.6 (CH, imidazole), 129.2 (CH, imidazole), 119.5 (CH, imidazole), 107.1 (2 x CH, Ar), 106.3 (2 x CH, Ar), 98.9 (CH, Ar), 98.8 (CH, Ar), 60.4 (2 x CH_2), 58.4 (CH), 58.1 (2 x CH_2), 55.3 (4 x OCH_3), 52.3 (2 x CH_2). [ES-HRMS] calculated for $\text{C}_{26}\text{H}_{35}\text{N}_4\text{O}_4$: 467.2653 $[\text{M}+\text{H}]^+$. Found: 467.2641 $[\text{M}+\text{H}]^+$.

4.3. Spectral Binding assay

CYP121A1 protein was expressed and purified as described previously.³⁰ Ligand binding assays were performed by spectrophotometric titration using a Cary 60 UV-visible scanning spectrophotometer (Agilent, UK) and a 1 cm path length quartz cuvette, recording spectra between 250 and 800 nm. Titrations were done with 3-4 μM CYP121A1 at 28 °C in 100 mM potassium phosphate (KPi) buffer, 200 mM KCl, pH 7.85 with 0.004% Triton X-100. Ligand stocks solutions were prepared in dimethylsulfoxide (DMSO). Ligands were added in successive small volumes (typically 0.05-0.2 μL aliquots) from concentrated stock solutions to the protein in a 1 mL final volume. Spectral measurements were taken before ligand addition, and following addition of each aliquot of ligand. Difference spectra at each stage in the titration were obtained by subtraction of the initial ligand-free enzyme spectrum from subsequent spectra collected after each addition of ligand. From the difference spectra, a pair of wavelengths were identified and defined as the absorbance maximum (A_{peak}) and minimum (A_{trough}). The overall absorbance change (A_{max}) was calculated by subtracting the minimum from the maximum absorbance for every spectrum collected after each aliquot addition. Graphs of (A_{max} , $\Delta\Delta\text{Absorbance}$) against [ligand] were plotted for each ligand. Titrations were repeated in triplicate and the final K_d value was determined from the average values across the three sets. The K_d values were determined from these plots of $\Delta\Delta\text{Absorbance}$ against ligand

concentration, and by fitting the data using either a standard hyperbolic function (Equation 1) or the Hill equation (Equation 2) using Origin software (OriginLab, Northampton, MA).

$$A_{\text{obs}} = (A_{\text{max}} * L / (K_d + L)) \quad (\text{Equation 1})$$

In Equation 1 (the standard hyperbolic function, essentially the Michaelis-Menten function adapted for ligand binding), A_{obs} is the observed absorbance change at ligand concentration L , A_{max} is the maximal absorbance change observed at ligand saturation, and K_d is the dissociation constant for the binding of the ligand (the substrate concentration at which $A_{\text{obs}} = 0.5 \times A_{\text{max}}$).

$$A_{\text{obs}} = (A_{\text{max}} \times L^n) / (K^n + L^n) \quad (\text{Equation 2})$$

In equation 2 (the sigmoidal Hill equation), A_{obs} is the observed absorbance change at ligand concentration L , A_{max} is the absorbance change at ligand saturation, K is the apparent dissociation constant, and n is the Hill coefficient, a value describing the apparent extent of cooperativity observed in ligand binding.

4.4. EPR Spectroscopy

Continuous wave X-band EPR spectra of ligand-free CYP121A1 (110 μM) as well as for CYP121A1 in complex with compounds from Series A, B and C (2 mM) were recorded using a Bruker ELEXSYS E500 EPR spectrometer with an ER 4122SHQ Super High Q cavity. Temperature was controlled with an ESR900 cryostat (Oxford Instruments, Abingdon UK). Spectra were recorded at 10 K, microwave power at 0.5 mW, modulation frequency 100 kHz and modulation amplitude at 7 G. Samples were prepared in 100 mM HEPES, 100 mM NaCl with 0.004% Triton X-100 at pH 7.6. Ligands were added from concentrated stock solutions in DMSO to a final concentration of 2 mM and samples incubated for 20 min at room temperature.

Samples were centrifuged briefly to remove any particulate matter prior to transfer to EPR tubes and freezing in liquid nitrogen.

4.5. Antimycobacterial Activity Assay

M. tuberculosis H₃₇Rv was grown in 7H9 liquid medium with 10% OADC enrichment. The bacteria growth occurred at 37°C until reaching the mid-log phase (OD_{600nm}=0.4-0.6). After this period, the bacterial suspensions were prepared as described below and REMA assays were performed. The anti-*M. tuberculosis* activity of the compounds was determined by the REMA (Resazurin Microtiter Assay) method.²⁰ Stock solutions of the tested compounds (10 µg/mL) were prepared in DMSO and diluted in Middlebrook 7H9 broth supplemented with 10% of OADC (OADC enrichment - BBL/Becton-Dickinson, Sparks, MD, USA).

The microdilution of the compounds was performed in 96-well plates to obtain final compound concentration ranges of 0.39-100 µg/mL. Rifampicin in a concentration range of 0.004-1 µg/mL was added as control. Bacterial suspensions were prepared and their turbidities adjusted to match the optical density of McFarland no.1 standard. After further dilution of 1:20 in the respective Middlebrook 7H9 broth supplemented with OADC, 100 µL of the inoculum was added to each well of the 96-well plate. Cultures were incubated for 7 days at 37°C, and 30 µL of 0.01% resazurin were added. Wells were read after 24 h for colour change and measured as the fluorescence (excitation/emission of 530/590 nm filters respectively) in a microfluorimeter. The MIC was defined as the lowest concentration resulting in 90% inhibition of *M. tuberculosis* growth. The presented results are from two independent experiments.

4.6. CYP121A1 Crystallography

Untagged CYP121A1 protein and crystals were prepared as previously reported, with the following adaptations.³⁰ Crystals were prepared using a Mosquito pipetting robot

(Molecular Dimensions, Newmarket, UK) in 800 nL drops with protein-to-mother liquor at a ratio of 1:1, by vapor diffusion in 1.5–2.1 M ammonium sulfate and 0.1 M sodium MES or Cacodylate from pH 5.5–6.15. Co-crystals were prepared following incubation with 2mM ligand prepared in DMSO. Protein solutions were centrifuged at 14,000 rpm for 20 mins at 4 °C immediately before crystallogenesis. Ligand soaks were also carried out either by directly dissolving solid ligand at saturation or by the addition of a 2–5 mM ligand solution in DMSO to the mother liquor, and soaking was carried out for a minimum period of 24 h. Crystals were immersed in mother liquor supplemented with 10-30% oil as cryoprotectant and cryoprotected and flash-cooled in liquid nitrogen. Data were collected on beamline i02 (wavelength 0.9795 Å) at the Diamond Light Source Facility (Oxfordshire, UK). The diffraction data were reduced, scaled and merged using XDS³¹ or Xia2³². Structures were refined using PHENIX³³ with the native CYP121A1 structure (PDB 1N40)³⁰ as the starting model. Structural rebuilding and validation were performed with COOT,³⁴ Molprobity³⁵ and PDB REDO,³⁶ Data collection and final refinement statistics are provided in Table 3. Images for presentation were rendered using an academic version of the PyMOL Molecular Graphics System, Schrödinger, LLC.

4.7. Molecular modeling.

4.7.1. Flexible alignment

Ligands **17** and the natural substrate cYY were built using MOE¹⁴ builder, and saved in a database. Each ligand and cYY were extracted from the database and energy minimisation was performed using the MMFF94 forcefield. Flexible alignment was performed for each ligand with cYY, giving an output database. The score functions were given for each pair that quantifies the quality of the alignment in terms of both internal strain and overlap of molecular features.

4.7.2. Docking studies

Docking studies were performed on an Intel Xenon ® CPU E5462 @ 280GHz x 4 processors running Linux Ubuntu 12.04.1 LTS using molecular operating environment (MOE) software¹⁴ and Mtb CYP121A1 co-crystallized with the natural substrate cYY at a resolution of 1.4 Å (PDB ID: 3G5H). All minimisations were performed with MOE to a RMSD gradient of 0.01 Kcal/mol/Å with MMFF94 forcefield, and partial charges were automatically calculated. The charge of the heme iron at physiological pH was set to 3⁺ (geometry d2sp3) through the atom manager in MOE. The Alpha Triangle placement, which derives poses by random superposition of ligand atom triplets through alpha sphere dummies in the receptor site, was chosen to determine the poses. The London ΔG scoring function estimates the free energy of binding of the ligand from a given pose. Refinement of the results using MMFF94 forcefield, and rescoring of the refined results using the London ΔG scoring function was applied. The output database dock file was created with different poses for each ligand and arranged according to the final score function (S), which is the score of the last stage that was not set to zero.

Acknowledgements

We thank the Egyptian Government for a Channel research scholarship to Hend Abd El-wahab and the EPSRC Mass Spectrometry Centre, Swansea, U.K. for mass spectroscopy data. For Leonardo Marino we thank his funders FAPESP (2011/21232-1); CNPQ (140079/2013-0) and CAPES PDSE (99999.003125/2014-09). Andrew Munro and Kirsty McLean are grateful for support for their research through grants from the BBSRC (Grant Nos. BB/K001884/1 and BB/I019227/1)

References

- (1) Dheda, K.; Barry, C.E.; Maartens, G. Tuberculosis. *Lancet* **2015**, *387*, 1211-1226.
- (2) World Health Organization. *Tuberculosis*. Fact sheet No. 104: <http://www.who.int/mediacentre/factsheets/fs104/en/> **2017** (accessed 5/8/17).
- (3) The National Institute for Health and Care Excellence. *Tuberculosis pathway*. London: NICE: <http://pathways.nice.org.uk/pathways/tuberculosis> **2015** (accessed 5/8/17).
- (4) McLean, K.J.; Dunford, A.J.; Neeli, R.; Driscoll, M.D.; Munro, A.W. Structure, function and drug targeting in *Mycobacterium tuberculosis* cytochrome P450 systems. *Arch. Biochem. Biophys.* **2007**, *464*, 228-240.
- (5) Park, D.K.; Lee, K.E.; Baek, C.H.; Kim, I.H.; Kwon, J.H.; Lee, K.H.; Kim, B.S.; Choi, S.H.; Kim, K.S. Cyclo(Phe-Pro) modulates the expression of ompU in *Vibrio* spp. *J. Bacteriol.* **2016**, *188*, 2214–2221.
- (6) Scopel, M.; Abraham, W.R.; Henriques, A.T.; Macedo, A.J. Dipeptide cis-cyclo(leucyl-tyrosyl) produced by sponge associated *Penicillium* sp. F37 inhibits biofilm formation of the pathogenic *Staphylococcus epidermidis*. *Bioorg. Med. Chem. Lett.* **2013**, *23*, 624–626.
- (7) Taubert, D.; Grimberg, G.; Stenzel, W.; Schömig, E. Identification of the endogenous key substrates of the human organic cation transporter OCT2 and their implication in function of dopaminergic neurons. *PLoS One* **2007**, *2*(4):e385.
- (8) Belin, P.; Le Du, M.H.; Fielding, A.; Lequin, O.; Jacquet, M.; Charbonnier, J.B.; Lecoq, A.; Thai, R.; Courçon, M.; Masson, C.; Dugave, C.; Genet, R.; Pernodet, J.L.; Gondry, M. Identification and structural basis of the reaction catalyzed by CYP121, an essential cytochrome P450 in *Mycobacterium tuberculosis*. *Proc. Nat. Acad. Sci. U.S.A.* **2009**, *106*, 7426-7431.

- (9) Fonvielle, M.; Le Du, M.H.; Lequin, O.; Lecoq, A.; Jacquet, M.; Thai, R.; Dubois, S.; Grach, G.; Gondry, M.; Belin, P. Substrate and reaction specificity of *Mycobacterium tuberculosis* cytochrome P450 CYP121: insights from biochemical studies and crystal structures. *J. Biol. Chem.* **2013**, *288*, 17347-17359.
- (10) Vinh, T. K.; Ahmadi, M.; Lopez Delgado, P. O.; Fernandez Perez, S.; Walters, H. M.; Smith, H. J.; Nicholls, P. J.; Simons, C. 1-[(Benzofuran-2-yl)phenylmethyl]-triazoles and - tetrazoles - potent competitive inhibitors of aromatase. *Bioorg. Med. Chem. Lett.* **1999**, *9*, 2105–2108.
- (11) Saberi, M. R.; Shah, K.; Simons, C. Benzofuran- and furan-2-yl-(phenyl)-3-pyridylmethanols: synthesis and inhibition of P450 aromatase. *J. Enzyme Inhib. Med. Chem.* **2005**, *20*, 135–141.
- (12) Gomaa, M.S.; Bridgens, C.E.; Veal, G.J.; Redfern, C.P.F.; Brancale, A.; Armstrong, J.L.; Simons, C. Synthesis and biological evaluation of 3-(1*H*-imidazol- and triazol-1-yl)-2,2-dimethyl-3-[4-(naphthalen-2-ylamino)phenyl]propyl derivatives as small molecule inhibitors of retinoic acid 4-hydroxylase (CYP26). *J. Med. Chem.*, **2011**, *54*, 6803-6811.
- (13) Kim, H.J.; Kwak, W.Y.; Min, J.P.; Lee, J.Y.; Yoon, T.H.; Kim, H.D.; Shin, C.Y.; Kim, M.K.; Choi, S.H.; Kim, H.S.; Yang, E.K.; Cheong, Y.H.; Chae, Y.N.; Park, K.J.; Jang, J.M.; Choi, S.J.; Son, M.H.; Kim, S.H.; Yoo, M.; Lee, B.J. Discovery of DA-1229: a potent, long acting dipeptidyl peptidase-4 inhibitor for the treatment of type 2 diabetes. *Bioorg. Med. Chem. Lett.* **2011**, *21*, 3809-3812.
- (14) Ott, I.; Kircher, B.; Heinisch, G. Substituted pyridazino[3,4-*b*][1,5]benzoxazepin-5(6*H*)ones as multidrug-resistance modulating agents. *J. Med. Chem.* **2004**, *47*, 4627-4630.
- (15) Zhang, C.; Tan, C.; Zu, X.; Zhai, X.; Liu, F.; Chu, B.; Ma, X.; Chen, Y.; Gong,

- P.; Jiang, Y. Exploration of (s)-3-aminopyrrolidine as a potentially interesting scaffold for discovery of novel abl and pi3k dual inhibitors. *Eur. J. Med. Chem.* **2011**, *46*, 1404-1414.
- (16) Das, S.; Das, V. K.; Saikia, L.; Thakur, A. J. Environment-friendly and solvent-free synthesis of symmetrical bis-imines under microwave irradiation. *Green Chem. Lett. Rev.* **2012**, *5*, 457-474.
- (17) Sharma, V.; Khan, M. S. Y. Synthesis of novel tetrahydroimidazole derivatives and studies for their biological properties. *Eur. J. Med. Chem.* **2001**, *36*, 651-658.
- (18) McLean, K.J.; Marshall, K.R.; Richmond, A.; Hunter, I.S.; Fowler, K.; Kieser, T.; Gurcha, S.S.; Besra, G.S.; Munro, A.W. Azole antifungals are potent inhibitors of cytochrome P450 mono-oxygenases and bacterial growth in mycobacteria and streptomycetes. *Microbiology* **2002**, *148*, 2937-2949.
- (19) Korzekwa, K. R.; Krishnamachary, N.; Shou, M.; Ogai, A.; Parise, R. A.; Rettie, A. E.; Gonzalez, F. J.; Tracy, T. S. Evaluation of atypical cytochrome P450 kinetics with two-substrate models: evidence that multiple substrates can simultaneously bind to cytochrome P450 active sites. *Biochemistry* **1998**, *37*, 4131-4147.
- (20) Palomino, J.C.; Martin, A.; Camacho, M.; Guerra, H.; Swings, J.; Portaels, F. Resazurin microtiter assay plate: simple and inexpensive method for detection of drug resistance in *Mycobacterium tuberculosis*. *Antimicrob. Agents Chemother.* **2002**, *46*, 2720-2722.
- (21) Ghose, A.K.; Crippen, G.M. Atomic physicochemical parameters for three-dimensional-structure-directed quantitative structure-activity relationships. 2. Modeling dispersive and hydrophobic interactions. *J. Chem. Inf. Comput. Sci.* **1987**, *27*, 21-35.

(22) *Molecular Operating Environment (MOE)*, 2013.08; Chemical Computing Group Inc., 1010 Sherbooke St. West, Suite #910, Montreal, QC, Canada, H3A 2R7, **2016**.

(23) Hudson, S.A.; McLean, K.J.; Surade, S.; Yang, Y.Q.; Leys, D.; Ciulli, A.; Munro, A.W.; Abell, C. Application of fragment screening and merging to the discovery of inhibitors of the *Mycobacterium tuberculosis* cytochrome P450 CYP121. *Angew. Chemie Int. Ed.* **2012**, *51*, 9311-9316.

(24) Kavanagh, M.E.; Gray, J.L.; Gilbert, S.H.; Coyne, A.G.; McLean, K.J.; Davis, H.J.; Munro, A.W. Substrate fragmentation for the design of *M. tuberculosis* CYP121 inhibitors. *ChemMedChem* **2016**, *11*, 1924-1935.

(25) Seward, H.E.; Roujeinikova, A.; McLean, K.J.; Munro, A.W.; Leys, D. Crystal structure of the *Mycobacterium tuberculosis* P450 CYP121-fluconazole complex reveals new azole drug-P450 binding mode. *J. Biol. Chem.* **2006**, *281*, 39437-39443.

(26) Cole, S.T.; Brosch, R.; Parkhill, J.; Garnier, T.; Churcher, C.; Harris, D.; Gordon, S.V.; Eiglmeier, K.; Gas, S.; Barry, C.E. 3rd; Tekaia, F.; Badcock, K.; Basham, D.; Brown, D.; Chillingworth, T.; Connor, R.; Davies, R.; Devlin, K.; Feltwell, T.; Gentles, S.; Hamlin, N.; Holroyd, S.; Hornsby, T.; Jagels, K.; Krogh, A.; McLean, J.; Moule, S.; Murphy, L.; Oliver, K.; Osborne, J.; Quail, M.A.; Rajandream, M.A.; Rogers, J.; Rutter, S.; Seeger, K.; Skelton, J.; Squares, R.; Squares, S.; Sulston, J.E.; Taylor, K.; Whitehead, S.; Barrell, B.G. Deciphering the biology of *Mycobacterium tuberculosis* from the complete genome sequence. *Nature* **1998**, *393*, 537-544.

(27) Butts, C. P.; Jazdyk, M. D. S. Piperazine additions to C60-a facile approach to fullerene substitution. *Org. Biomol. Chem.* **2005**, *3*, 1209-1216.

(28) Li, Y.; Bacon, K.; Sugimoto, H.; Fukushima, K.; Hashimoto, K.; Marumo, M.; Moriwaki, T.; Nunami, N.; Tsuno, N.; Urbahns, K. 2-Phenoxy- and 2-

phenylsulfomamide derivatives with ccr3 antagonistic activity for the treatment of asthma and other inflammatory or immunological disorders. WO2004084898 A1, **2004**.

(29) Boyce, R.S.; Phillips, J.; Speake, J.D. Quinazolinone compounds with reduced bioaccumulation. WO2005051391 A1, **2005**.

(30) McLean, K.J.; Carroll, P.; Lewis, D.G.; Dunford, A.J.; Seward, H.E.; Neeli, R.; Cheesman, M.R.; Marsollier, L.; Douglas, P.; Smith, W.E.; Rosenkrands, I.; Cole, S.T.; Leys, D.; Parish, T.; Munro, A.W. Characterization of active site structure in CYP121. A cytochrome P450 essential for viability of *Mycobacterium tuberculosis*. H37Rv. *J. Biol. Chem.* **2008**, *283*, 33406-33416.

(31) Kabsch W. XDS. *Acta Crystallogr. Sect. D Biol. Crystallogr.* **66**, 125-32.

(32) Winter G. (2010) Xia2: an expert system for macromolecular crystallography data reduction. *J Appl Crystallogr.* **2010**, *43*, 186-90.

(33) Adams, P.D.; Afonine, P.V.; Bunkóczi, G.; Chen, V.B.; Davis, I.W.; Echols, N.; Headd, J.J.; Hung, L.-W.; Kapral, G.J.; Grosse-Kunstleve, R.W.; McCoy, A.J.; Moriarty, N.W.; Oeffner, R.; Read, R.J.; Richardson, D.C.; Richardson, J.S.; Terwilliger, T.C.; Zwart, P.H. Phenix: A comprehensive python-based system for macromolecular structure solution. *Acta Crystallogr. Sect. D Biol. Crystallogr.* **2010**, *66*, 213-221.

(34) Emsley, P.; Lohkamp, B.; Scott, W.G.; Cowtan, K. Features and development of Coot. *Acta Crystallogr. Sect. D Biol. Crystallogr.* **2010**, *66*, 486-501.

(35) Chen, V.B.; Arendall, W.B. 3rd; Headd, J.J.; Keedy, D.A.; Immormino, R.M.; Kapral, G.J.; Murray, L.W.; Richardson, J.S.; Richardson, D.C. MolProbity: all-atom structure validation for macromolecular crystallography. *Acta Crystallogr. Sect. D Biol. Crystallogr.* **2010**, *66*, 12-21.

(36) Joosten, R.P.; Long, F.; Murshudov, G.N.; Perrakis, A. The PDB_REDO server for macromolecular structure model optimization. *IUCrJ*. **2014**, *1*, 213-20.